NASA TECHNICAL NOTE

NASA TN D-2021

NASA TN D-2021

LATERAL-SPREAD SONIC-BOOM GROUND-PRESSURE MEASUREMENTS FROM AIRPLANES AT ALTITUDES TO 75,000 FEET AND AT MACH NUMBERS TO 2.0

by Domenic J. Maglieri, Tony L. Parrott, David A. Hilton, and William L. Copeland

Langley Research Center

Langley Station, Hampton, Va.

NATIONAL AERONAUTICS AND SPACE ADMINISTRATION • WASHINGTON, D. C. • NOVEMBER 1963

TECHNICAL NOTE D-2021

LATERAL-SPREAD SONIC-BOOM GROUND-PRESSURE MEASUREMENTS FROM AIRPLANES AT ALTITUDES TO 75,000 FEET AND AT MACH NUMBERS TO 2.0

By Domenic J. Maglieri, Tony L. Parrott, David A. Hilton, and William L. Copeland

Langley Research Center
Langley Station, Hampton, Va.

NATIONAL AERONAUTICS AND SPACE ADMINISTRATION

NATIONAL AERONAUTICS AND SPACE ADMINISTRATION

TECHNICAL NOTE D-2021

LATERAL-SPREAD SONIC-BOOM GROUND-PRESSURE MEASUREMENTS FROM AIRPLANES AT ALTITUDES TO 75,000 FEET AND AT MACH NUMBERS TO 2.0

By Domenic J. Maglieri, Tony L. Parrott, David A. Hilton, and William L. Copeland

SUMMARY

Measurements of shock-wave overpressures are presented for a wide range of altitudes and Mach numbers of fighter and bomber airplanes on the ground track and for lateral distances up to about 20 miles. Included also are measurements of wave angles, wave fronts, wavelengths, rise times, impulses, and reflection coefficients.

Lift effects were apparent for the bomber airplane for a wide range of altitudes but were noted to be much less significant for the fighter airplanes. For the fighter airplanes, measured values of shock-wave overpressures, wavelength, and positive and negative impulses were in good agreement with calculations based on theory which accounts only for volume effects. For the bomber airplane, however, sizable discrepancies were noted between measurements and volume-theory calculations, and these are believed to be due to associated lift effects. Some significant atmospheric effects were noted with regard to the angles of incidence of the shock waves at ground level and with regard to the shapes of the wave fronts. The measured lateral extent of the ground pressure pattern is in general agreement with calculations based on atmospheric refraction considerations.

INTRODUCTION

The sonic boom is an important consideration in the planning of military training missions and supersonic-transport routes. The width of the sonic-boom ground intersection pattern is important because it will determine the area exposed during a particular flight. For flights in the vicinity of large populated areas, there may be a requirement to minimize the sonic-boom exposure by lateral displacement of the airplane. Thus, the width of the pattern and the lateral pressure distribution for various flight conditions are required in order to establish an acceptable lateral distance.

A considerable amount of information, both theoretical and experimental, is available with regard to sonic-boom exposures nearly underneath airplanes. Such data have been reported for a variety of operating conditions and for both small

and large airplanes, as for instance references 1 to 11. Only a few reliable lateral pressure measurements have been reported, and these are mainly for a limited range of altitudes and for fighter airplanes. A limited amount of lateral-spread experimental data for an airplane for which lift effects are known to be significant was reported in reference 1. Although analytical procedures for predicting lateral pressure distributions including effects of lift (ref. 12) have been proposed, no calculations of this type have been published to date.

In the present study, data were obtained under closely controlled flight conditions for a range of altitudes up to about 75,000 feet. In addition, measurements were made at distances out to 20 miles in the lateral direction at several measuring stations, the records of which were time synchronized to provide some information on the shape of the ground intersection patterns. Of particular interest is the fact that data were obtained for a bomber airplane for which it has been demonstrated that lift effects are important. Special instrumentation was used to preserve the true pressure signatures at the ground and in free air so that they might be studied in detail.

The purpose of this paper is to present the data from a special series of flight tests and to correlate the results with some unpublished results of previous flight tests. The data presented are believed to be useful directly for planning purposes and, in addition, will be useful for comparison with future analytical developments.

SYMBOLS

A	airplane cross-sectional area, sq ft
d	lateral distance measured perpendicular to airplane ground track, miles
h	vertical distance from ground to airplane flight path, ft
I	pressure impulse obtained by integrating pressure signature, lb-sec/sq ft
K_2	airplane body-shape factor
l	airplane length, ft
M	airplane Mach number
Δp	pressure rise across bow shock wave (overpressure), lb/sq ft
Δp_o	measured pressure rise across shock wave at ground level, lb/sq ft
S	distance, parallel to ground track, from plane perpendicular to ground and containing airplane to a point on the intersection of Mach cone and ground plane (as defined in fig. 16)

s_l distance, parallel to ground track, from plane perpendicular to ground plane and containing vertex of hyperbola, formed by intersection of ray-path cone with ground plane, to the hyperbola at a given lateral distance (as defined in fig. 7)

s_t distance, parallel to ground track, from plane perpendicular to ground plane and containing airplane to plane perpendicular to ground plane and containing vertex of hyperbola, formed by intersection of ray-path cone with ground plane (as defined in fig. 7)

$s = s_t + s_l$

Δt time interval between bow and tail shock waves of airplane measured in horizontal plane at ground level, sec

X distance between bow and tail shock waves of airplane measured in horizontal plane at ground level (wavelength), ft

x cylindrical coordinate measured along body axis, ft

λ rise time (time for ambient pressure to rise to maximum peak overpressure value), sec

μ Mach angle, $\sin^{-1}\frac{1}{M}$

ϕ experimentally determined shock-wave angle, deg

Subscripts:

calc calculated

exp experimental

pos positive

neg negative

APPARATUS AND METHODS

Most of the information reported in the present paper relates to test flights accomplished in the vicinity of Edwards Air Force Base supersonic flight corridor and in the area just east of Rogers Dry Lake, Edwards, Calif., during September and October 1961. (See fig. 1.) Airplane A (without external pod) and airplane B (see fig. 2) were used in the Edwards studies.

Also included is a limited amount of previously unpublished data from other flight studies involving airplane A (with external pod) and airplanes C and D (see fig. 2). Unless otherwise noted, the following detailed discussions of procedures and results relate to the Edwards studies.

Test Conditions

The Edwards terrain is generally flat with only sparse vegetation and is at an altitude of 2,000 to 3,000 feet above sea level. As can be seen from figure 1, no extreme variations in elevation existed in the test area.

The ground instrumentation was located in a T-shaped array with 10 microphone locations being in a line parallel to the center line of the supersonic flight corridor and extending a distance of about 4 miles. This instrumentation was alined along the heading of 245°-65° magnetic. Additional microphone stations and microbarographs provided and operated by Sandia Corporation, Albuquerque, N. Mex., were located at lateral distances of about $1\frac{1}{2}$, 5, 10, and 20 miles and were alined generally perpendicular to the arrangement along the ground track. (See fig. 1.) The main recording station was located near the intersection of the two instrument arrangements. The accurate locations of all stations were established by means of standard surveying and optical techniques.

Test Arrangements

Photographs of the types of airplanes from which data are presented are shown in figure 2, and some additional descriptive information is contained in table I. The normal cross-sectional-area distributions for all test airplanes are given in figure 3. The area distribution for airplane C was obtained from line drawings of the airplane. It should be noted that airplane A was operated both with and without the detachable external pod. Airplanes A, B, and C were provided, maintained, and operated by U.S. Air Force personnel, whereas airplane D was maintained and operated by NASA personnel.

Airplane Positioning

The airplanes, in all cases, were positioned over the test area by means of ground-control procedures with the aid of radar tracking. Radar plotting-board overlays were obtained for all flights, and the data obtained at 1-second intervals were used to provide information of the type shown in figure 4. For steady flight conditions the data of the plotting-board overlay, from which plan position, altitude, and speed can be obtained, were of sufficient accuracy for purposes of the tests.

All of the present data were obtained at sustained steady flight conditions within the capabilities of the particular airplane involved with the exception of those involving the bomber airplane at altitudes above 70,000 feet. In order to stabilize altitude over the required portion of the flight track for altitudes above 70,000 feet, the Mach number was allowed to decrease slowly as a function

of time (about M = 0.10 in 10 miles). For these latter conditions, zoom-type maneuvers were resorted to for the purpose of obtaining the test altitude. In order to synchronize the tracking data with all ground pressure measurements, a 1,000-cps tone signal was superposed on the data records at the time the airplane passed over the main recording station.

Atmospheric Soundings

Rawinsonde observations from the Edwards Air Force Base weather facility, which was located within about 9 miles of the main recording station, were taken within 3 hours of the times of all test flights. Measured values of temperature and pressure, along with the calculated speed of sound and humidity values and wind velocity and direction values, were provided at 1,000-foot intervals to altitudes of about 5,000 feet in excess of the airplane test altitude. Samples of the atmospheric pressure, temperature, and speed-of-sound data for some of the test flights, along with the ICAO standard atmospheric values for comparison (see ref. 13), are shown plotted as a function of altitude in figure 5. Wind velocity has been resolved into components parallel to and perpendicular to the airplane flight path, and sample data are shown in figure 6. Pressure, temperatures, and relative humidity data were obtained with wiresonde equipment during the times of the tests at altitudes up to about 1,000 feet as described in reference 1.

It was found in general that for altitudes up to the tropopause the atmospheric pressure, temperature, and speed of sound were generally higher than those of the ICAO standard atmosphere. The wind profiles shown in figure 6 were obtained during soundings in which maximum wind velocities of about 80 to 90 feet per second were recorded for the test period.

Ground-Pressure Instrumentation

The ground-pressure instrumentation provided and operated by the NASA consisted of an arrangement of special microphones located in an area measuring approximately 4 by 20 miles. The main recording station was arranged in such a manner that the signals from 11 of the microphones could be recorded simultaneously on magnetic tape. A vertical arrangement of two microphones (one at ground level and the other one at a height of 30 feet directly above) was used to indicate the true shock-wave angle at ground level. In addition to the main station arrangement, a satellite station with up to two microphone channels was mounted in a vehicle which could be positioned at various test locations within a 20-mile radius of the main station. Five measuring stations with microbarograph equipment were provided by Sandia Corporation. One of these stations was located in the same area as the main microphone recording station, and the others were located at distances of about 5, 10, and 20 miles from the main station in a direction generally perpendicular to the supersonic flight corridor.

The data were obtained during the tests of reference 1, and hence the same instrumentation, calibrations, mounting schemes, operating techniques, wind screen equipment, instrument check-outs, and record synchronization were used as are reported in reference 1.

In addition to the NASA and Sandia instrumentation, use was made of a specially instrumented range in the test area (see fig. 1) in order to get data relating to a better definition of the wave-front ground intersections. This latter instrumentation consisted of eight geophones and microphones located accurately within an area roughly 4,000 feet by 4,000 feet. The output signals of these microphones and geophones were simultaneously recorded and were synchronized with the recordings of the NASA stations in order to provide accurate shock-wave arrival time information.

Flight-Test Procedures

It should be remembered that a sonic-boom disturbance on the ground under the airplane flight track is measured after the airplane passes over the measuring point, but is generated at a point in space several miles up along the flight track. Thus, for sonic-boom measurements at a given point on the ground, it is important that suitable flight conditions be maintained in the vicinity of the generating point in space. It follows, then, that if simultaneous measurements are to be made over an area on the ground, the corresponding flight conditions must be maintained for a specified distance along the flight track. This portion of stabilized flight will be referred to as the "data acquisition zone." Thus, for any given flight tests, it is important to determine the location and extent of this data acquisition zone so that measurements over an area on the ground will be valid. The location and extent of the data acquisition zone are a function of the airplane operating conditions, of Mach number and altitude, and the position of the flight track relative to the measuring station as illustrated in figure 7.

Figure 7 consists of schematic diagrams showing both profile- and plan-view ray paths for low and high Mach numbers. The data of the figure apply only to the bow wave for convenience and are further simplified to apply only to the conditions of a homogeneous atmosphere with zero wind. Since there are no speed-of-sound gradients in this atmosphere between the airplane and the ground, the bow wave as indicated schematically in the figure would extend to the ground in a straight line at an angle μ determined by the flight Mach number. This bow wave would then propagate perpendicular to itself in the direction of the ray path (dashed line) at approximately the speed of sound. The diagram in the upper left-hand side of the figure applies to a low Mach number, steady flight condition. The airplane generated the disturbance that is observed at the point p_0 while it was at a distance s_t up the track over point p_1. This distance s_t is a function of the height and Mach number of the airplane and is given by the following expression:

$$s_t = \frac{h}{\sqrt{M^2 - 1}}$$

It is important to note that all of the disturbances that radiate from the airplane when it is over point p_1 intersect the ground to form a hyperbola as indicated in the bottom sketch. It can be seen that the ground intersection at point p_2 is at a greater horizontal distance than p_0 by the amount s_l. The

quantity s_l is a function of the lateral distance d as well as airplane Mach number and height, as defined in the following equation:

$$s_l = \frac{\sqrt{d^2 + h^2} - h}{\sqrt{M^2 - 1}}$$

The distance s defined as $s_t + s_l$ represents the minimum horizontal distance measured along the ground track between the measuring station and the airplane position for valid comparative measurements during stabilized flight.

It can be seen that for low Mach numbers at a given altitude and at large lateral distances d, the total distance s is large relative to s_l for high Mach number cases as illustrated in figure 7(b). It is believed that for the conditions of the present tests the atmospheric effects were generally small compared with the geometric effects, but in all cases would tend to make the critical distance values larger than those calculated from the previously given expressions.

RESULTS AND DISCUSSION

The two main types of information obtained in the present studies were (a) detailed pressure-time histories and (b) arrival times of the shock waves. These data were obtained during the course of the studies of reference 1 wherein there were more measuring stations on the ground track than at the various lateral locations. (See fig. 1.) Hence, more data are presented in this paper for locations along the track than for lateral locations. During the course of the measurements, care was taken in selecting the instrumentation to preserve the main features of the pressure signatures so that the various quantities defined in figure 8 could be evaluated. Determinations were made of such quantities as the ground overpressures Δp_o, the rise time λ, the positive impulse I_{pos}, the negative impulse I_{neg}, and the time duration Δt from which wavelength X was computed based on a knowledge of airplane speed.

Ground Overpressures at Lateral Stations

Measured ground and free-air overpressure values for both fighter and bomber airplanes are presented as a function of lateral distance in figures 9 and 10. Fighter airplane data are included for a Mach number range from 1.23 to 2.0 and an altitude range of 10,300 to 53,000 feet. Bomber airplane data are included for a Mach number range of 1.5 to 2.0 and an altitude range of 31,200 to 74,700 feet. These data are compared with calculated ground pressures based on volume considerations only (see refs. 3 and 4) for a reflection factor of 1.8 and for the geometric parameters given in table I. (No attempt is made to account for wake effects.) The associated calculated lateral cut-offs due to refraction in a standard atmosphere are also shown. (See ref. 5.)

The data for the fighter airplanes as shown in figure 9 are either in general agreement with the calculations or tend to be lower than the calculated values. The only exceptions are the data of figure 9(b) which are for airplane C. (Both ground and free-air measurements are shown along with a calculated ground pressure curve.) These data were obtained during flights over a large populated area and for low ambient temperatures, whereas all other data in figure 9 were measured in the vicinity of an unpopulated, dry lake area and for moderate temperatures. The reason the measured values of figure 9(b) exceed the theory in the manner shown is not understood, but it is believed to be associated with the peculiar temperature profiles which can exist over populated areas during the cold seasons.

No sharp cut-off due to refraction is evident although it is clear that because of a limited amount of equipment measurements were not detailed enough to properly define such a cut-off. In some cases the lateral pattern was noted to exist beyond the calculated cut-off distance as based on a standard atmosphere, and such results were associated with temperature inversion conditions of the lower atmosphere as were previously described in reference 7. There may also have been some cross-wind effects such as those described in reference 2. As a matter of interest, some free-air measurements and ground surface measurements at the same lateral location indicated essentially the same values of Δp. When this condition existed, the arrival times were also noted to be nearly identical, which suggests a vertical wave front and a near cut-off condition.

As shown in figure 10, the measured overpressure data for the bomber airplane fall generally higher than the calculated values and drop off in magnitude as a function of lateral distance at a faster rate. It should be noted that the measured data on the track were in better agreement with the combined lift-volume calculations than for volume-alone calculations as indicated in figure 20 of reference 1. Combined lift-volume overpressure calculations at lateral distances are not available for comparison. As in the case of the fighter airplanes, not enough data were obtained to define the cut-off points, and furthermore, the lateral measuring stations did not extend far enough to define the lateral extremity of the pattern for some flight conditions. As a matter of further interest, the data of figure 10(b), which were obtained at the same location and during the same season as those of figure 9(b), also show a similar lateral distribution pattern.

Tracings of some measured ground pressure signatures obtained at various lateral distances up to about 20 miles from the ground track for the bomber airplane A at an altitude of about 61,000 feet and at a Mach number of about 2.0 are presented in figure 11. Also presented in the figure are peak overpressures and time interval values measured for each test. The pressure signatures are seen to have the gross features of N-waves. At the larger lateral distances, however, they seem to have a more ragged appearance, possibly a result of atmospheric effects in propagation. A notable difference is that at the lateral distance locations (figs. 11(b), (c), and (d)), there is generally a relatively slow rise time λ and a relatively slow return to atmospheric pressure as compared with the data of figure 11(a) which were obtained on the ground track. In general, the peak pressure values decrease gradually as the lateral distance increases, as was shown in figure 10. The time intervals, however, do not seem to vary in a systematic manner with increasing lateral distance as was the case for increasing altitude for the on-the-track condition. (See fig. 17 of ref. 1.)

Wavelength

Figure 12 presents a summary of the wavelength information obtained on the ground track for three different airplanes. The quantity Δt as defined in the sketch of figure 8 was measured directly in all cases and was used along with a knowledge of the airplane speed to calculate the wavelength X, which is assumed to be the distance between the bow and tail shock waves. Although data have been obtained for several other airplanes, only the results for three of the airplanes, for which a wide range of altitude data were obtained, are presented. The data for airplane B and airplane D are noted to be in good agreement with the calculated curves based on volume theory (ref. 4), and these calculated curves, in general, bracket the data points. In the case of the bomber airplane, however, the wavelength values exceed the calculated values based on volume theory, particularly at altitudes above 50,000 feet for which conditions it is known that lift effects are important. The data of the figure are plotted as a function of distance between the observer and the airplane. This distance is equal to the altitude of the airplane in all cases except for the square data points of the bomber airplane. These data were taken from probe flights as reported in reference 9.

Impulses

The impulse associated with the overpressure time history is a significant quantity relative to the manner in which building components respond to sonic booms. (See ref. 7.) The positive impulse is defined as the integral under the positive phase of the pressure time history, and likewise the negative impulse is defined as the integral under the negative portion of the pressure-time-history curve. The positive and negative impulses along the ground track have been evaluated for both fighter and bomber airplanes, and these data are presented in figure 13. In all cases, the measurements are compared with a simplified theory curve based on volume theory with the assumption that the wave is symmetrical; that is, the positive and negative impulses are equal. For the fighter airplanes, both positive and negative impulse values are in fairly good agreement with the predicted values over the range of altitudes for which data are shown. There is a trend for the positive impulses at the higher altitudes to exceed the calculated values and also to be larger than the measured negative impulse values. For the bomber airplane, both positive and negative values exceed the predicted values over the entire altitude range for which data are presented, and the positive impulse values tend to exceed the negative impulse values over the entire altitude range for which data are presented. This result suggests that lift effects are important for this airplane over the entire operating range. The fact that more scatter exists in the negative values than in the positive values results from the difficulty of determining the integral under the negative portion of the pressure curve, particularly at the aft end where some peculiar wake effects seem to exist. (See fig. 8.) The results previously discussed are consistent with those for in-flight probe measurements reported in reference 9.

From the time-history records obtained at various lateral stations (see fig. 11), the positive impulses have been evaluated for the bomber airplane A at

various lateral distances for various flight altitudes, and these data are presented in figure 14. Here again the measurements are compared with a simplified theory curve based on volume theory. The data points for the on-the-track condition are the average of the positive impulse values at the corresponding altitudes shown in figure 13. Examination of the results presented in figure 14 indicates that in general, the measured positive impulse values exceed the predicted values at all of the lateral measuring stations. This result again suggests that lift effects are important for this airplane over the entire operating range. The measured positive impulses would be expected to be higher at the lateral measuring stations because the measured overpressure values shown in figure 10 are larger than those predicted based on the volume theory, and also because the time intervals of the positive phase of the pressure signature appeared to increase slightly as a function of lateral distance. (See fig. 11.)

Wave Angles

With the aid of the vertical microphone array located on the ground track, in which the free-air microphone is located 30 feet directly above a ground microphone, it was possible to calculate from measured data the shock-wave angles ϕ. This calculation is based on a knowledge of the geometry of the microphone array, the airplane flight track, and the measured differences in the arrival times of the shock wave at the two microphones. If there are no temperature or wind gradients in the atmosphere between the airplane and the ground, the shock waves generated by the airplane would extend to the ground in a straight line at an angle determined by the flight Mach number. (See dashed line of insert sketch of fig. 15.) Data were obtained for both fighter and bomber airplanes for an altitude range of approximately 10,000 to 75,000 feet and for a Mach number range of about 1.1 to 2.0. These data are presented in figure 15 for the on-the-track condition and are compared with the predicted Mach angles as indicated by the solid curve. (See insert sketch of fig. 15.) It can be seen from the data of the figure that the shock-wave angles as determined from the measurements in general are 5° to 20° larger than the calculated Mach angles. This result would be expected for a normal temperature gradient. Wind gradients might either add to or subtract from the temperature-gradient effect, but for these experiments the wind effects apparently did not override the temperature. There seem to be no systematic differences between data obtained for morning and afternoon flights and for flights at widely different altitudes.

Wave Fronts

In addition to the effects already discussed, the atmospheric conditions also have an effect on the speed of propagation of the shock waves and, hence, the shape of the lateral-spread patterns. Information of this type was obtained by means of the lateral measuring stations and is presented in figure 16 (also reported in ref. 10) for two flights for which the atmospheric conditions were different.

The bow shock wave from the airplane intersects the ground plane in a manner indicated by the upper sketch in figure 16. The calculated ground intersection

curve on one side of the flight track, from an airplane flying in a homogeneous (no wind, constant temperature) atmosphere at a Mach number of 2 and at an altitude of 50,000 feet, is shown by the solid curve in the figure. It can be seen that when the airplane is in the overhead position the calculated bow wave intersection with the ground plane trails by about 16 miles along the track. Accurately measured arrival time information from stations at various lateral distances d perpendicular to the ground track interpreted in terms of distance S parallel to the ground track is listed in table II, and some of these data for flight conditions comparable to those of the calculations are also plotted in figure 16 for comparison.

The filled points represent data obtained for a headwind gradient condition for which the maximum wind velocity at an altitude of 50,000 feet was about 50 ft/sec. The open points represent data for a tailwind gradient of about the same magnitude. Both sets of data were obtained within a 10-minute time interval. It is obvious from the figure that the measured shapes of the wave fronts in the nonhomogeneous atmosphere did not differ markedly from the wave front calculated for the homogeneous atmosphere. The measured wave front represented by the filled symbols is located ahead of the wave front represented by the open symbols. This would be expected since the wind and temperature effects are additive for a headwind gradient condition and tend to oppose each other for a tailwind gradient condition. (See, for example, wind gradients of fig. 6.) The fact that both sets of data lie ahead of the calculated curve suggests that wind effects are relatively small for these tests as compared with other effects of nonhomogeneity such as temperature gradient. The differences shown are larger, however, than can be accounted for by calculations in which attempts are made to include the effects of temperature gradient.

As a matter of further information, the data of the lower sketch of the figure which were obtained with the aid of the closely spaced microphones and geophones over about a 1-mile segment of the range are presented. Local translations of the wave front of about 100 feet were observed over this 1-mile distance. These "ripples" in the wave front are believed to be associated with local variations of the atmosphere.

Reflection Coefficients

For a large number of overpressure measurements in the vicinity of the ground tracks of the airplanes, the reflection coefficients from the ground were very nearly equal to 2.0. It should be pointed out that the ground surface, which was a dry lake bed, was flat and very hard. This value is somewhat higher than has been reported from other field tests (see, for example, ref. 3), but it is believed that the differences are related to the nature of the respective ground surfaces in the test areas. At the extreme distance for which measurements were made in a lateral direction from the flight track, there was evidence that the reflection coefficient decreased to a value approaching 1.0. This was determined from the fact that measurements on the ground and on top of a 100-foot tower gave essentially the same overpressure values. (See figs. 9 and 10.) Furthermore, the arrival times at these two measuring points were nearly the same, which suggests that the shock wave was nearly perpendicular to the reflecting surface as

it passed by. This result is consistent with measured data of reference 11 for flights at low Mach numbers. For the present tests, the shock waves were perpendicular to the reflecting surface because of the Mach number and because of the geometry of the Mach cone in the vicinity of the ground reflection plane at large lateral distances. (See sketch of fig. 16.)

Rise Times

Since the rise time λ of the wave as defined in figure 8 may be a significant factor in community response, the opportunity was taken to evaluate this quantity for a range of flight conditions for the bomber airplane, and these data are presented in figure 17. All data presented were measured on the ground track, and an attempt has been made to normalize the data by dividing through by the corresponding overpressure Δp_o. This parameter is shown as a function of altitude. It can be seen that there is considerable scatter, but in general the rise time based on unit ground overpressure increases as the altitude of the airplane increases. It can be seen from a study of the pressure signature of figure 8 that the onset of pressure is very sudden, followed by a nearly vertical rise, and then a later gentle rounding off at the positive pressure peak. This positive peak is not generally sharply defined, probably because of atmospheric effects, and hence part of the scatter of figure 17 is due to the method of evaluation.

SUMMARY OF RESULTS

Measurements of shock-wave arrival times and overpressures for both fighter and bomber airplanes in the Mach number range 1.1 to 2.0 and for altitudes from 10,000 to 75,000 feet for measuring stations both on the flight track and at lateral distances out to about 20 miles have been made and suggest the following conclusions:

1. Although some scatter in the data was noted at large lateral distances, measured overpressures for both the fighter and bomber airplanes were maximum on the flight track and decreased generally with increasing lateral distance. A comparison with volume theory calculations indicated that the fighter airplane data were in good agreement with the theory in the vicinity of the flight track and as predicted by theory decreased in magnitude with increasing lateral distance at about the same rate. For the bomber airplane, the measured data on the track were markedly higher than the values calculated by volume theory but drop off in magnitude with increasing lateral distance at a relatively faster rate than the calculated values. It is believed that these results point up the fact that the lift effects are more significant for the bomber airplane than for the fighter airplanes and, furthermore, that the lift effects are most significant at locations along and near the ground track.

2. With regard to the lateral extent of the ground pressure pattern, data were not detailed enough to properly define the cut-off experimentally. The results, however, are in general agreement with those predicted by theory on the basis of atmospheric refraction. The limited data available do not indicate a sudden decrease in the pressures near the cut-off point as suggested by theory.

3. The measured time intervals between the bow and tail waves for the fighter airplanes were in good agreement with predicted values. The bomber time intervals, however, were generally larger than the predicted values, particularly for the higher altitudes for which condition it is known that lift effects are relatively more important.

4. Both positive and negative impulses determined from measured data for the fighter airplanes were in good agreement with those predicted from volume theory. Similar data for the bomber airplane were markedly higher than the predicted values.

5. The atmospheric effects were noted to be such as to increase the angles of incidence of the waves at the ground and to cause relatively small ripples in the wave fronts. No large distortions of the wave fronts were detected.

6. Ground reflection coefficients on the airplane ground track varied between 1.8 and 2.0, whereas at extreme lateral distances there was evidence that the reflection coefficient decreased to a value approaching 1.0.

7. Although considerable scatter existed in the data, the rise times generally increased as the airplane altitude increased.

Langley Research Center,
National Aeronautics and Space Administration,
Langley Station, Hampton, Va., August 9, 1963.

REFERENCES

1. Hubbard, Harvey H., Maglieri, Domenic J., Huckel, Vera, and Hilton, David A.: Ground Measurements of Sonic-Boom Pressures for the Altitude Range of 10,000 to 75,000 Feet. NASA TM X-633, 1962.

2. Lina, Lindsay J., Maglieri, Domenic J., and Hubbard, Harvey H.: Supersonic Transports - Noise Aspects With Emphasis on Sonic Boom. 2nd Supersonic Transports (Proceedings). S.M.F. Fund Paper No. FF-26, Inst. Aero. Sci., Jan. 25-27, 1960, pp. 2-12.

3. Maglieri, Domenic J., Hubbard, Harvey H., and Lansing, Donald L.: Ground Measurements of the Shock-Wave Noise From Airplanes in Level Flight at Mach Numbers to 1.4 and at Altitudes to 45,000 Feet. NASA TN D-48, 1959.

4. Whitham, G. B.: The Behavior of Supersonic Flow Past a Body of Revolution, Far From the Axis. Proc. Roy. Soc. (London), ser. A, vol. 201, no. 1064, Mar. 7, 1950, pp. 89-109.

5. Randall, D. G.: Methods for Estimating Distributions and Intensities of Sonic Bangs. R. & M. No. 3113, British A.R.C., 1959.

6. Maglieri, Domenic J., and Hubbard, Harvey H.: Ground Measurements of the Shock-Wave Noise From Supersonic Bomber Airplanes in the Altitude Range From 30,000 to 50,000 Feet. NASA TN D-880, 1961.

7. Maglieri, Domenic J., Huckel, Vera, and Parrott, Tony L.: Ground Measurements of Shock-Wave Pressure for Fighter Airplanes Flying at Very Low Altitudes and Comments on Associated Response Phenomena. NASA TM X-611, 1961.

8. Reed, Jack W.: Microbarograph Measurements and Interpretations of B-58 Sonic Booms, Project Big Boom. SC-4634(RR), Sandia Corp. (Albuquerque, N. Mex.), Dec. 1961.

9. Maglieri, Domenic J., Ritchie, Virgil S., and Bryant, John F., Jr.: In-Flight Shock-Wave Pressure Measurements Above and Below a Bomber Airplane at Mach Numbers From 1.42 to 1.69. NASA TN D-1968, 1963.

10. Maglieri, Domenic J., and Parrott, Tony L.: Atmospheric Effects on Sonic-Boom Pressure Signatures. Sound, vol. 2, no. 4, July-Aug. 1963, pp. 11-14.

11. Lina, Lindsay J., and Maglieri, Domenic J.: Ground Measurements of Airplane Shock-Wave Noise at Mach Numbers to 2.0 and at Altitudes to 60,000 Feet. NASA TN D-235, 1960.

12. Walkden, F.: The Shock Pattern of a Wing-Body Combination, Far From the Flight Path. Aero. Quarterly, vol. IX, pt. 2, May 1958, pp. 164-194.

13. Minzner, R. A., Ripley, W. S., and Condron, T. P.: U.S. Extension to the ICAO Standard Atmosphere - Tables and Data to 300 Standard Geopotential Kilometers. Geophys. Res. Dir. and U.S. Weather Bureau, 1958.

TABLE I.- TEST AIRPLANE CHARACTERISTICS

Airplane	Type	Length, ft	Wing area, sq ft	Gross weight, lb	K_2
A	Bomber	96.8	1,542	63,000 to 116,000	0.62
B	Fighter	54.7	196	20,000 to 25,000	.60
C	Fighter	70.8	631	30,000 to 36,000	.60
D	Fighter	58.8	452	30,000 to 35,000	.56

TABLE II.- DEFINITION OF THE GROUND INTERSECTION PATTERN OF THE BOW SHOCK WAVE FOR AIRCRAFT IN SUPERSONIC FLIGHT AT VARIOUS ALTITUDES AND MACH NUMBERS

Airplane altitude, ft (a)	Mach number	S_{exp}, mile	S_{calc}, mile	S_{exp}, mile	S_{calc}, mile	S_{exp}, mile	S_{calc}, mile	S_{exp}, mile	S_{calc}, mile
		d = 0 mile		d = 5 miles		d = 10 miles		d = 20 miles	
21,700	1.35	3.13	3.73	3.79	6.00	6.93	9.03	-----	-----
21,800	1.11	1.20	1.97	1.77	3.22	3.47	5.19	-----	-----
22,000	1.23	1.65	3.00	2.65	4.80	5.37	7.95	-----	-----
31,200	1.50	5.82	6.14	7.24	8.35	10.64	12.76	19.52	23.24
32,200	1.34	3.22	5.05	4.45	7.17	7.28	10.85	-----	-----
32,800	1.69	7.48	7.83	9.56	10.54	14.01	15.71	25.78	28.15
41,200	1.85	10.27	11.50	11.60	13.59	15.99	19.30	28.27	33.60
43,200	1.44	7.64	8.06	8.78	9.42	11.52	13.17	18.80	22.16
49,700	1.96	14.26	15.16	16.37	17.27	21.16	22.73	34.35	36.26
51,000	1.93	13.45	15.13	15.53	17.21	20.62	22.30	33.56	36.13
51,600	2.00	14.40	16.20	16.50	18.27	21.22	23.67	35.50	38.30
61,100	2.00	18.30	19.40	20.19	21.29	24.57	26.07	36.83	39.82
63,000	2.00	19.62	20.10	21.14	22.00	25.02	26.46	37.98	40.25
65,300	2.00	19.75	20.70	21.27	22.40	24.96	26.94	37.15	40.37
70,700	1.72	18.26	18.15	19.62	19.51	22.99	22.88	-----	33.35
72,000	1.60	16.62	16.50	17.19	17.28	18.02	20.63	-----	29.92
74,700	1.65	15.56	18.00	16.36	19.14	19.00	22.26	-----	31.82

[a]Altitude referred to mean sea level.

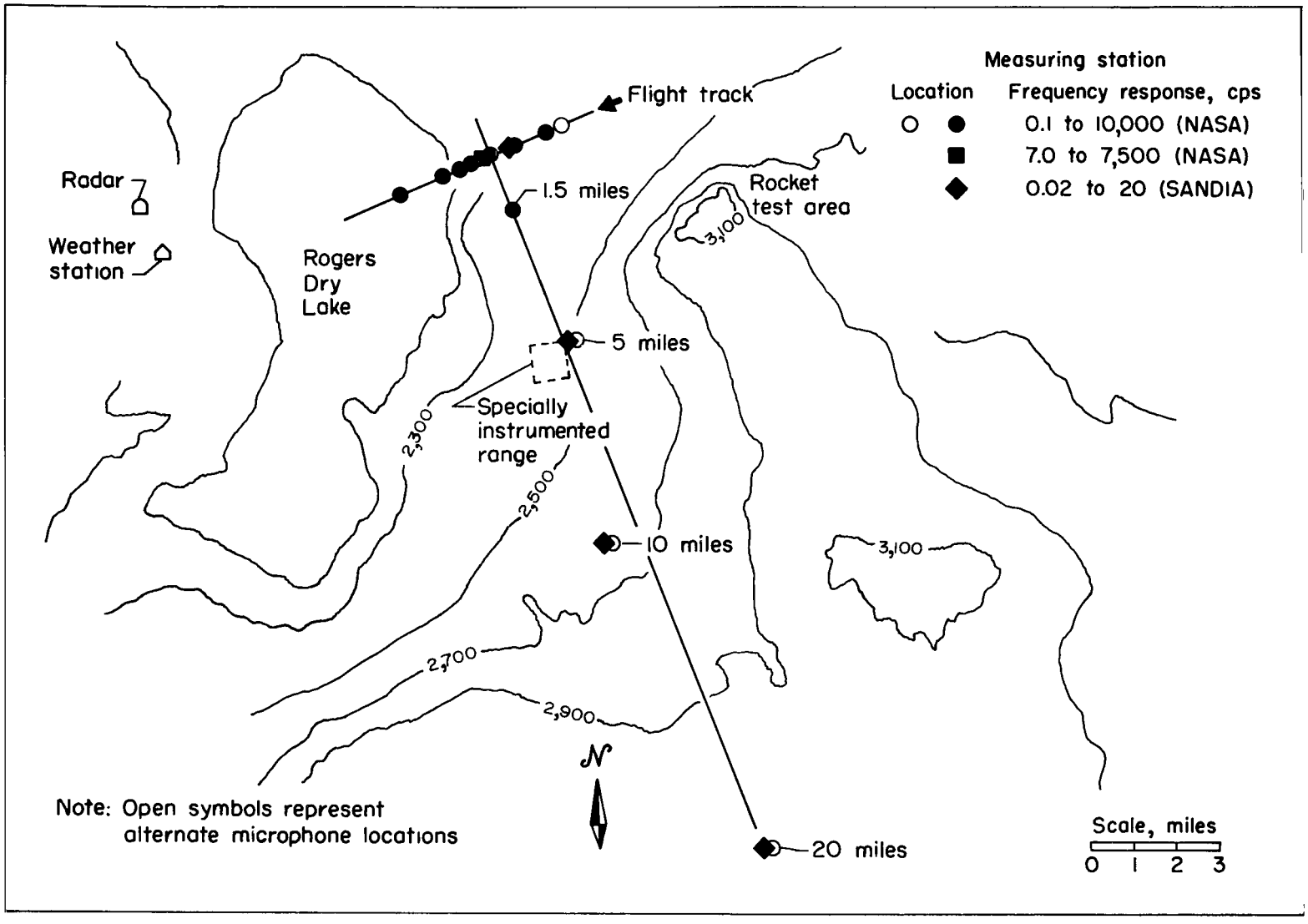

Figure 1.- Arrangement of facilities and equipment at the Edwards Air Force Base test site.

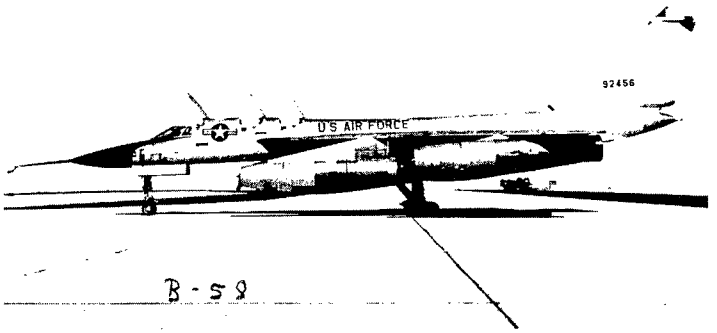

Airplane A

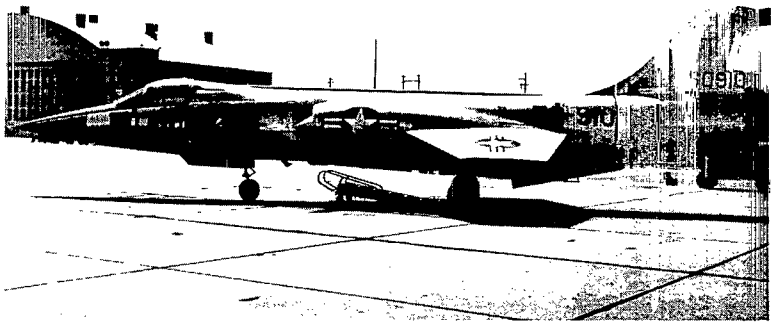

Airplane B

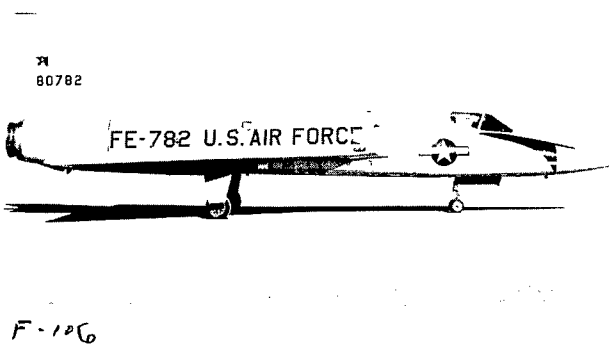

Airplane C

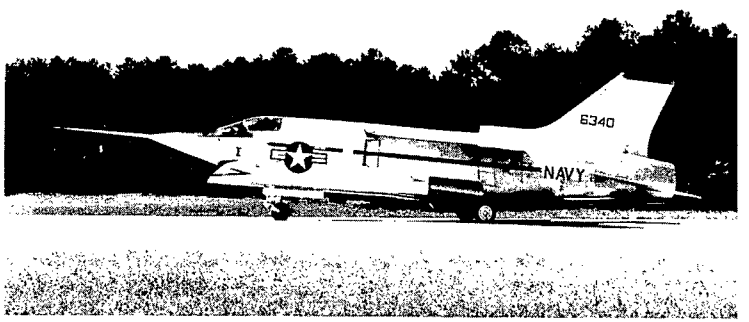

Airplane D

Figure 2.- Photographs of airplanes for which data are presented. L-63-4736

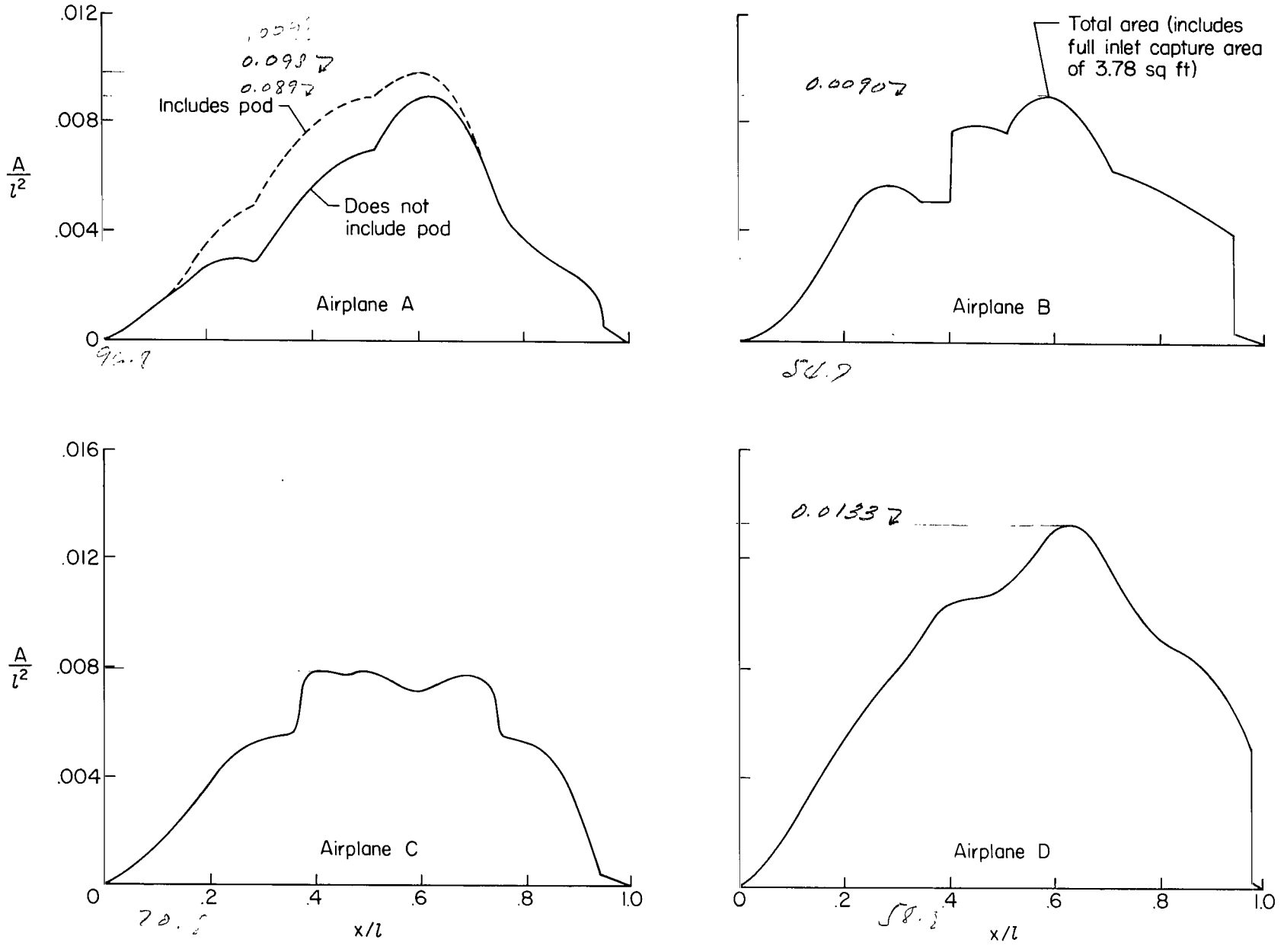

Figure 3.- Normal cross-sectional-area distributions of airplanes for which data are presented.

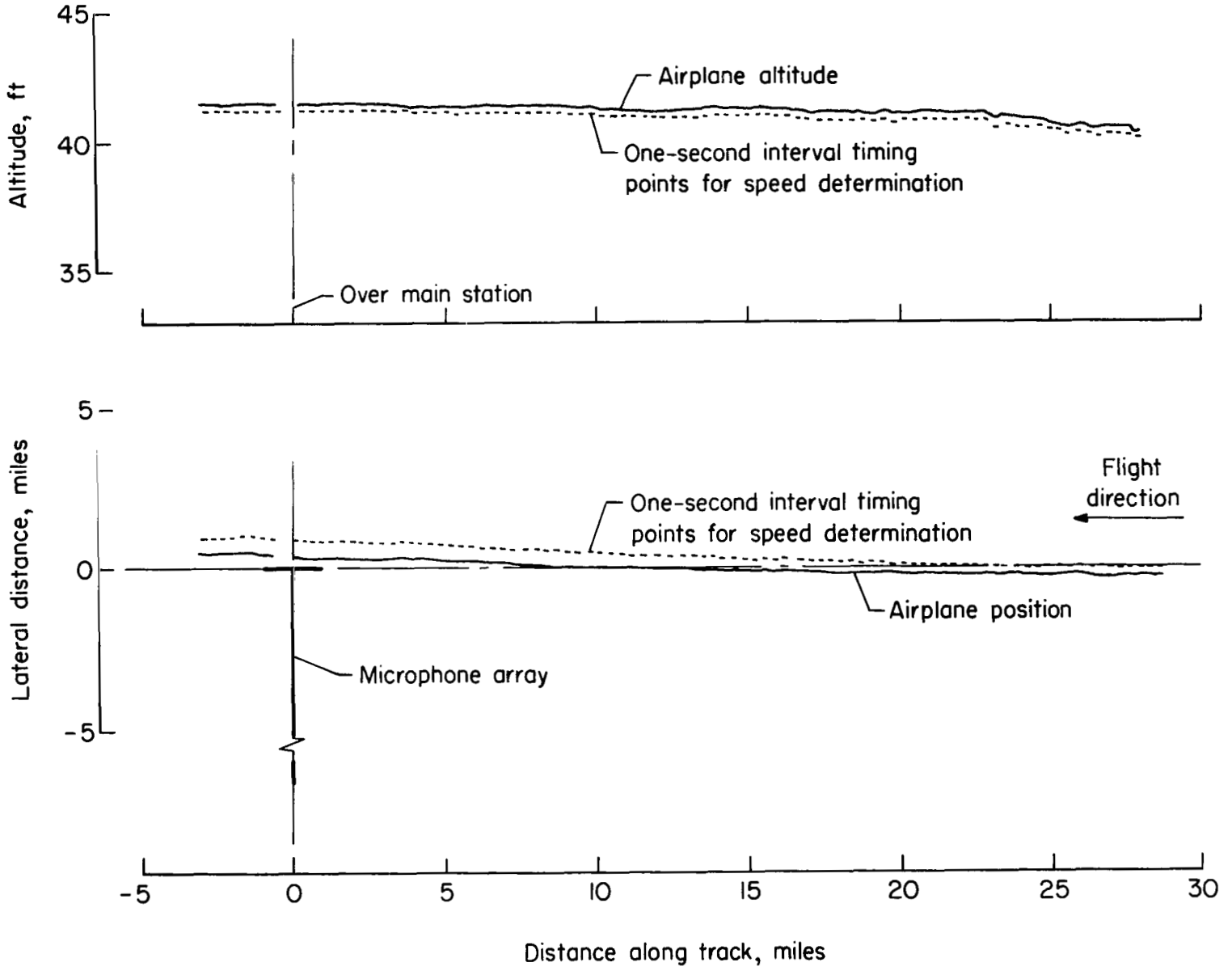

Figure 4.- Radar plotting-board track of airplane during steady level flight indicating both altitude and plan position as a function of time.

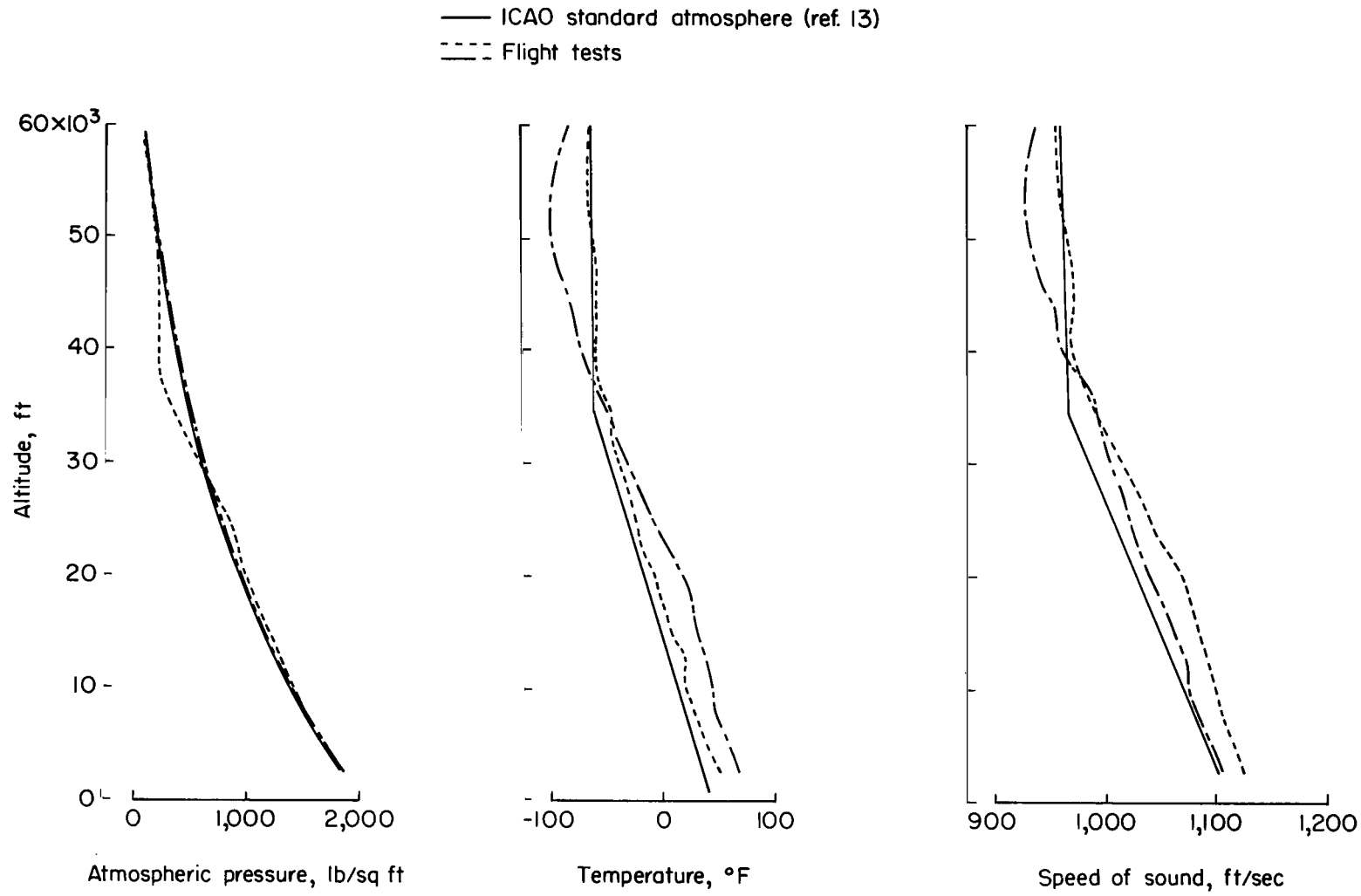

Figure 5.- Results from atmospheric soundings taken during flight tests.

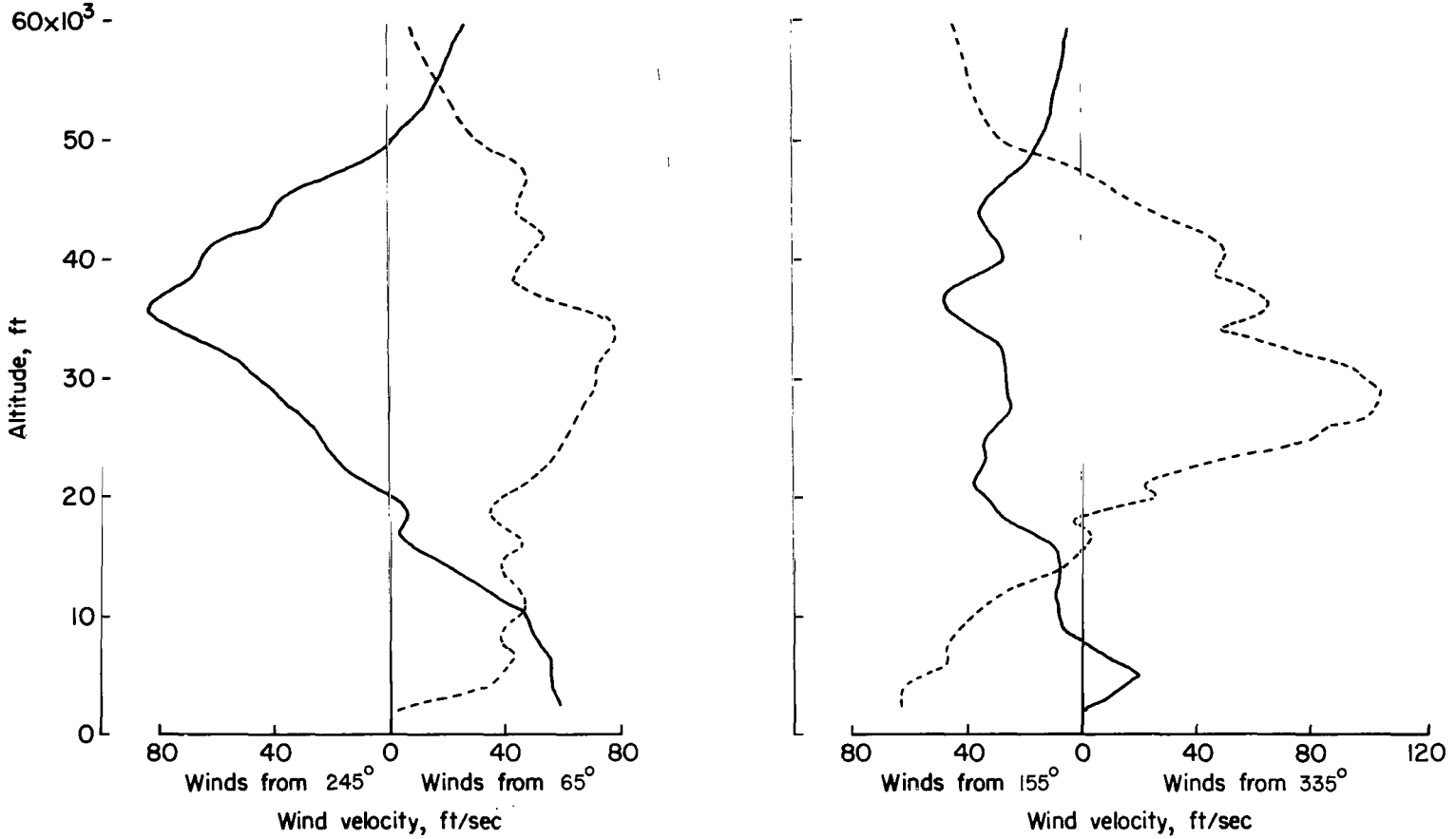

(a) Components along flight paths.

(b) Components perpendicular to flight paths.

Figure 6.- Wind data obtained from atmospheric soundings taken during flight tests.

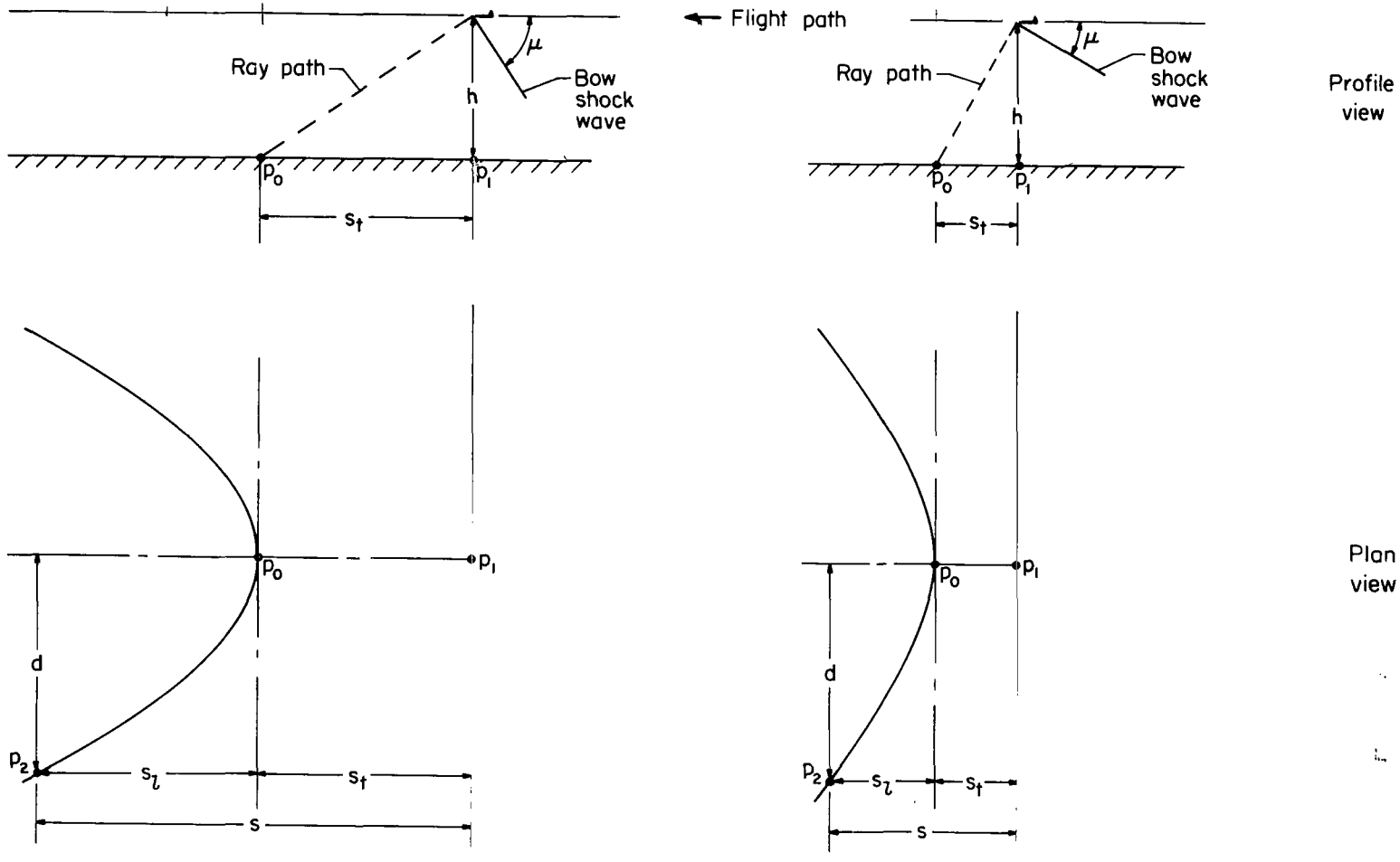

(a) Low Mach number.

(b) High Mach number.

Figure 7.- Schematic diagram showing profile- and plan-view ray paths for airplane at low and high Mach numbers.

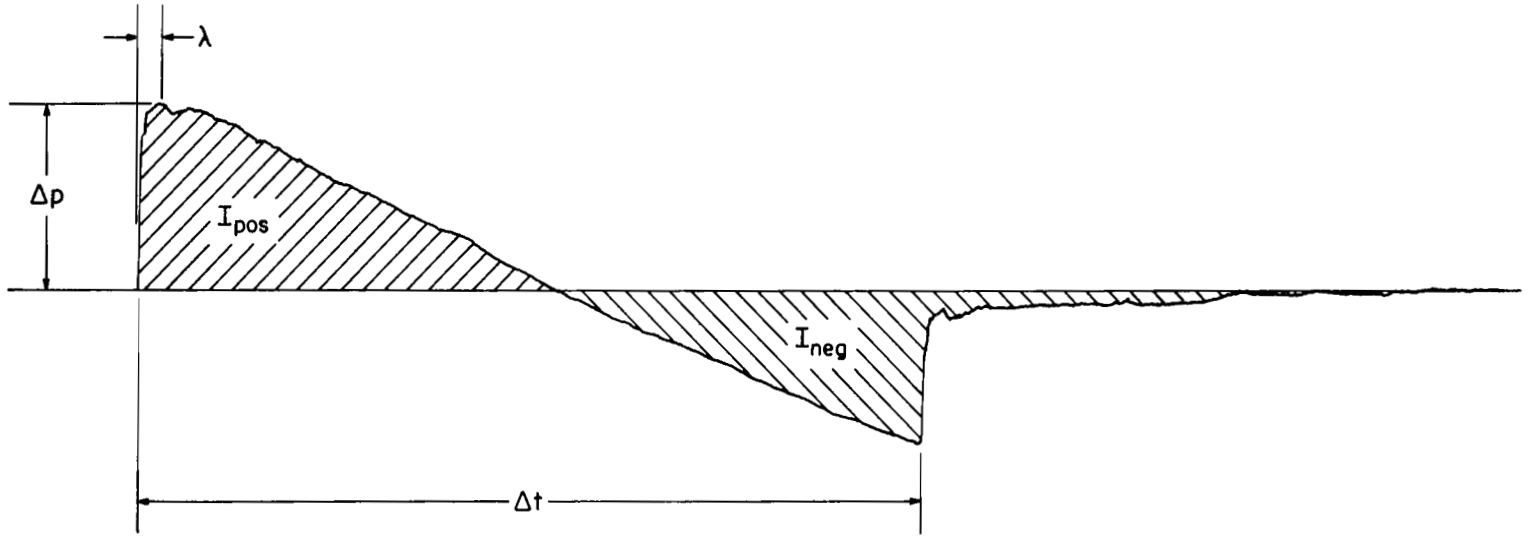

Figure 8.- Tracing of sonic-boom ground pressure signature on ground track for airplane A.

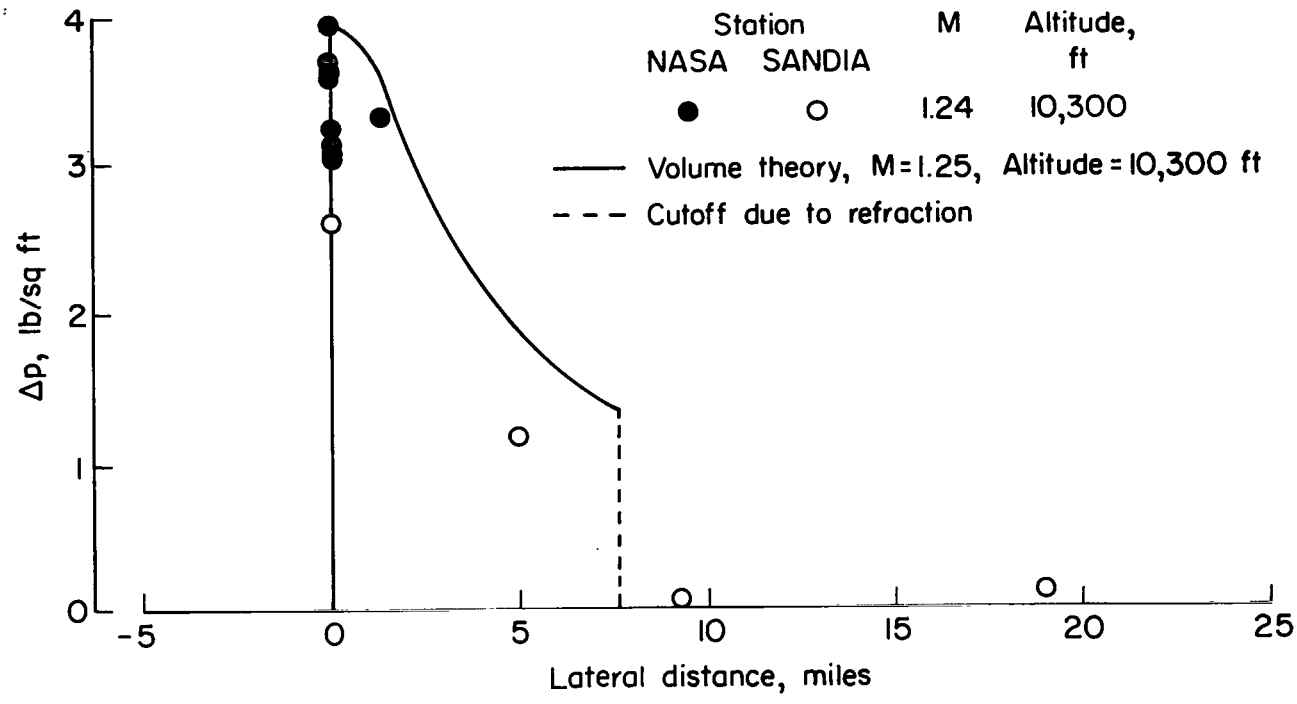

(a) Airplane B.

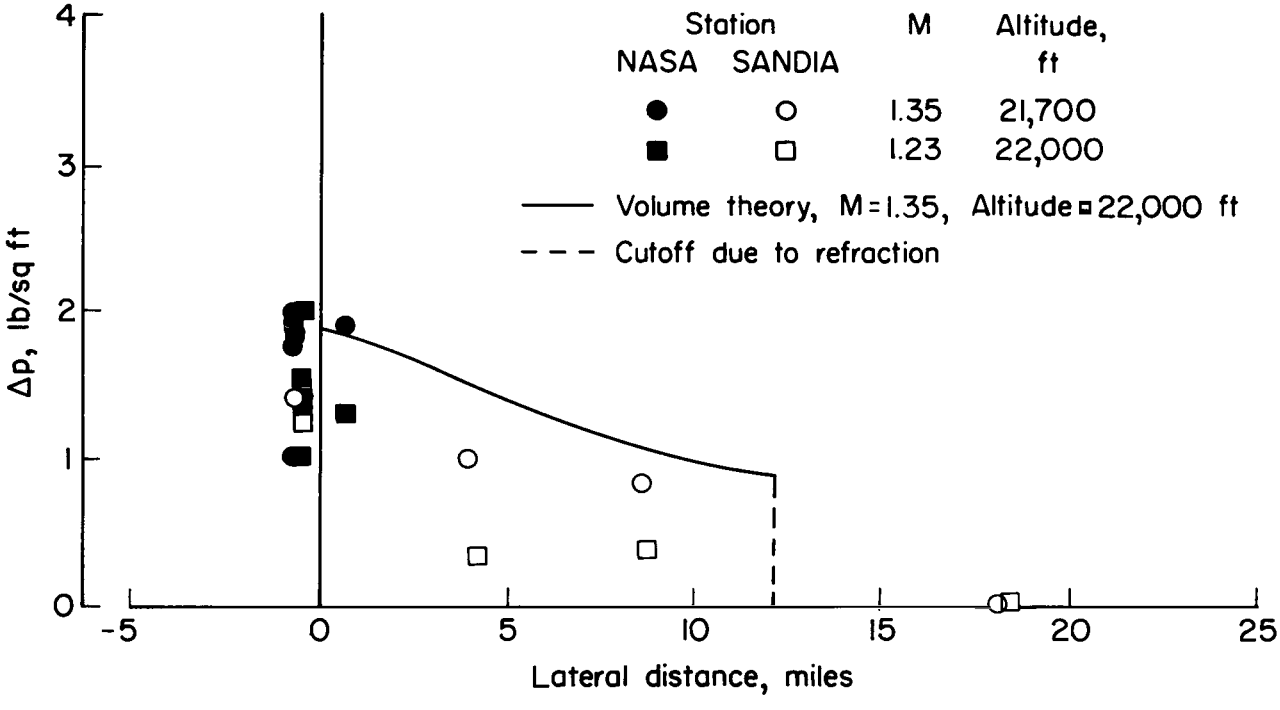

(a) Airplane B - Continued.

Figure 9.- Measured ground and free-air shock-wave overpressures for fighter airplanes for a range of altitudes and Mach numbers as a function of lateral distance from ground track.

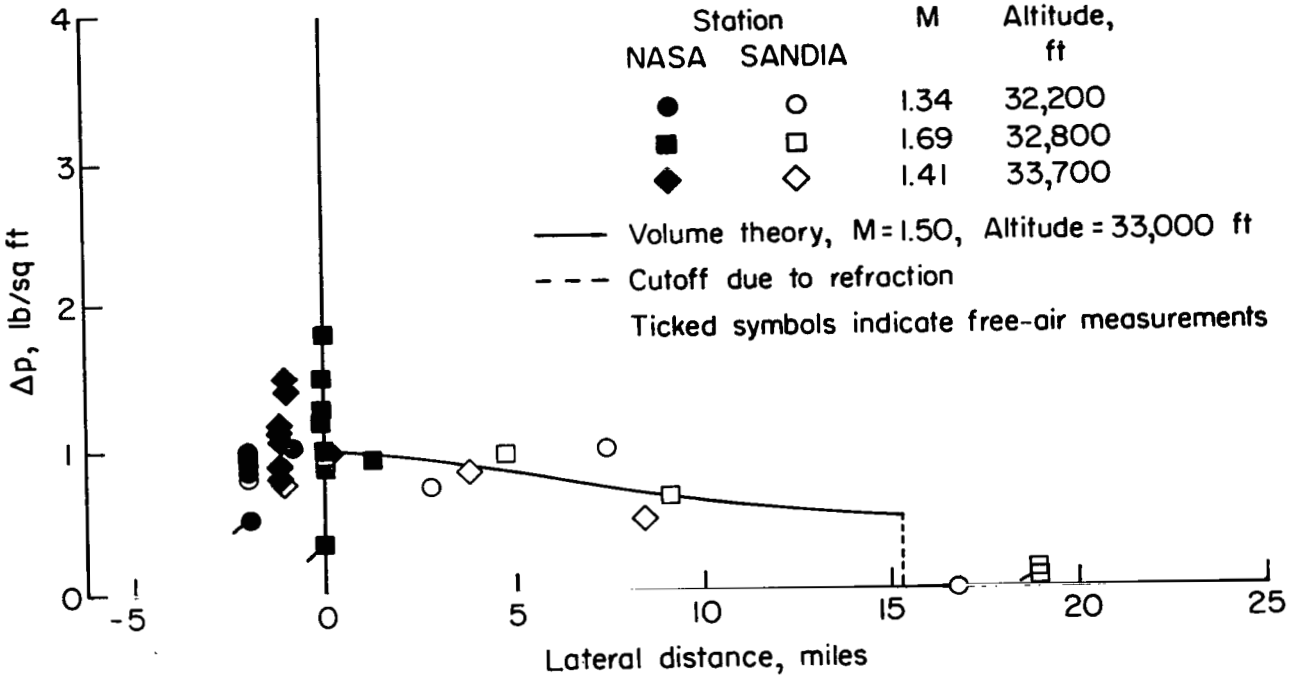

(a) Airplane B - Continued.

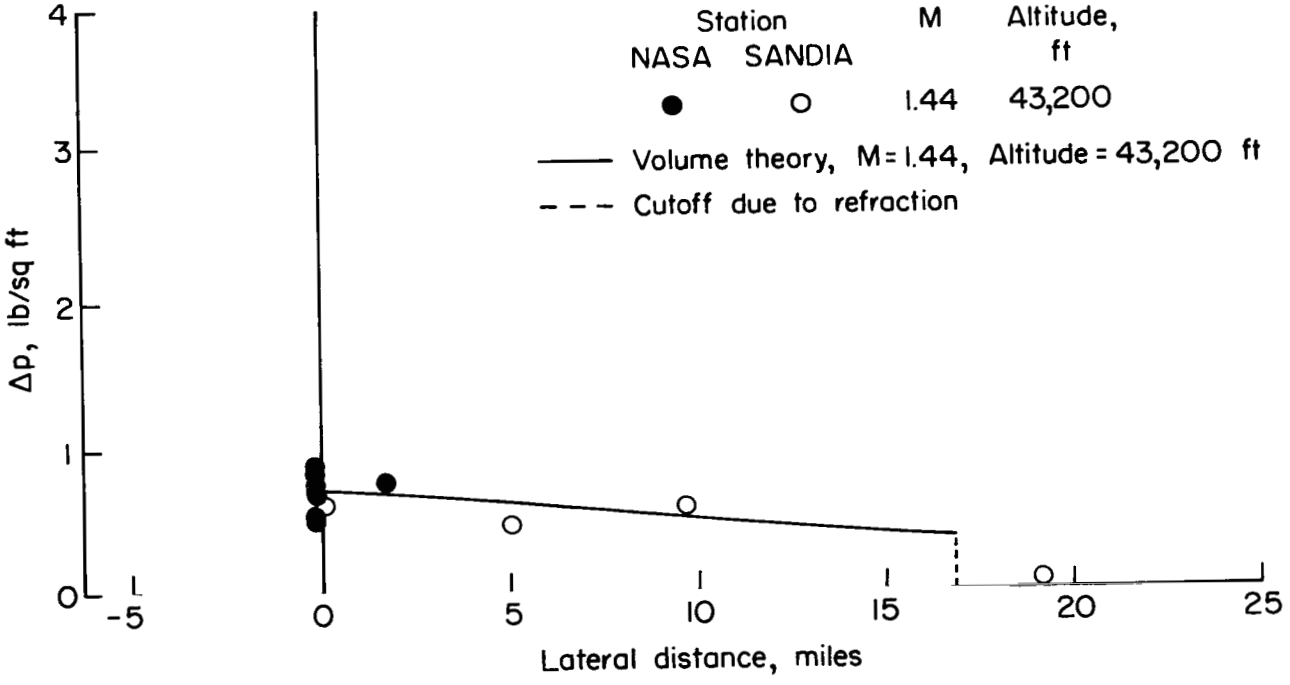

(a) Airplane B - Continued.

Figure 9.- Continued.

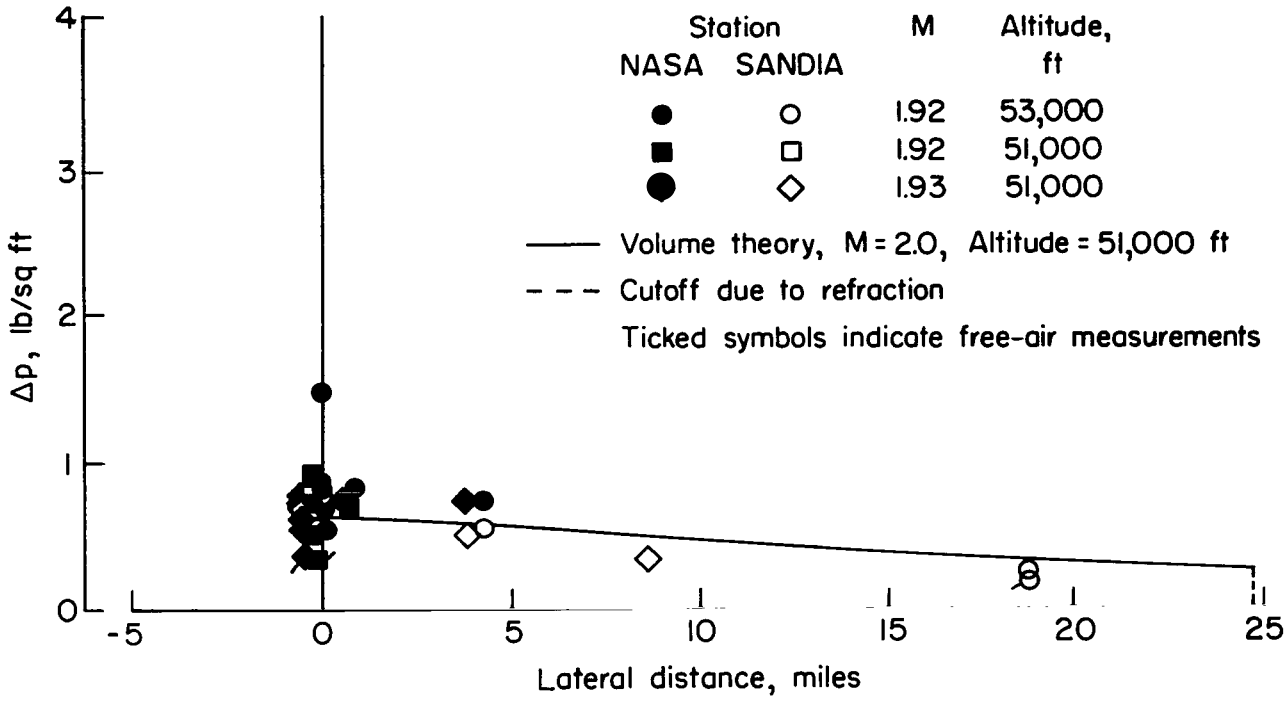

(a) Airplane B - Concluded.

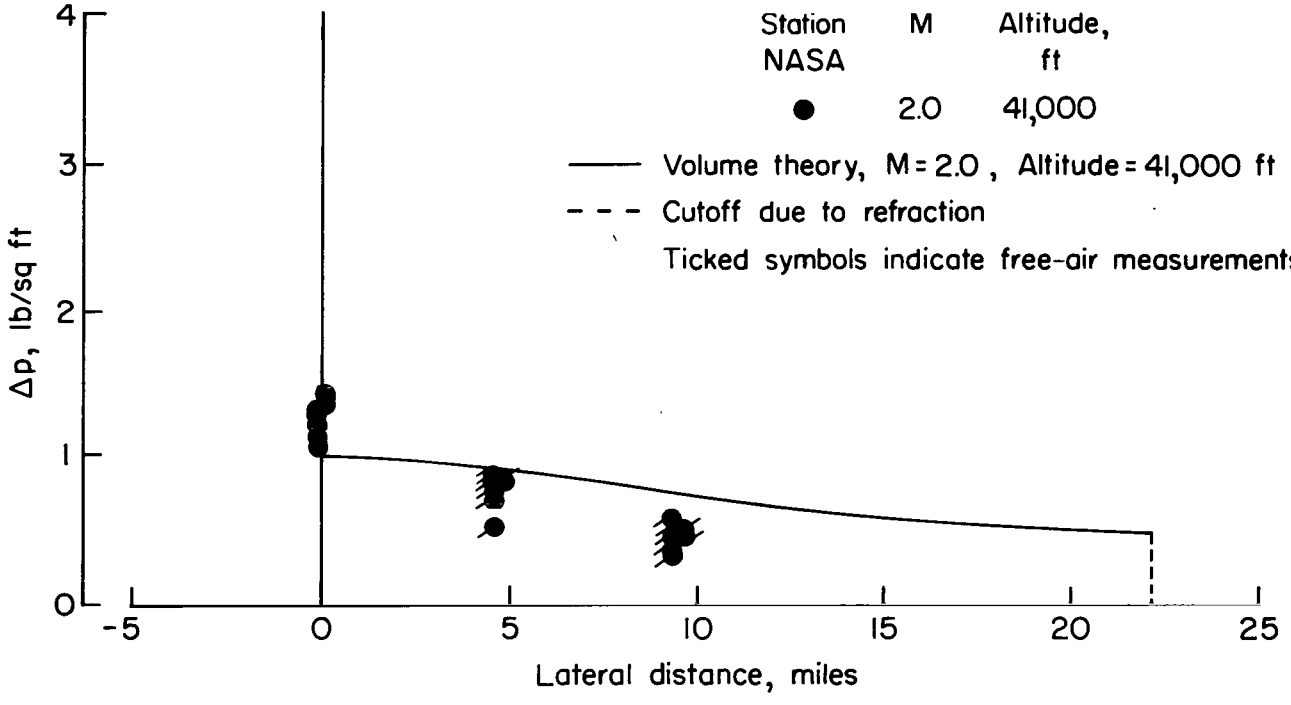

(b) Airplane C.

Figure 9.- Concluded.

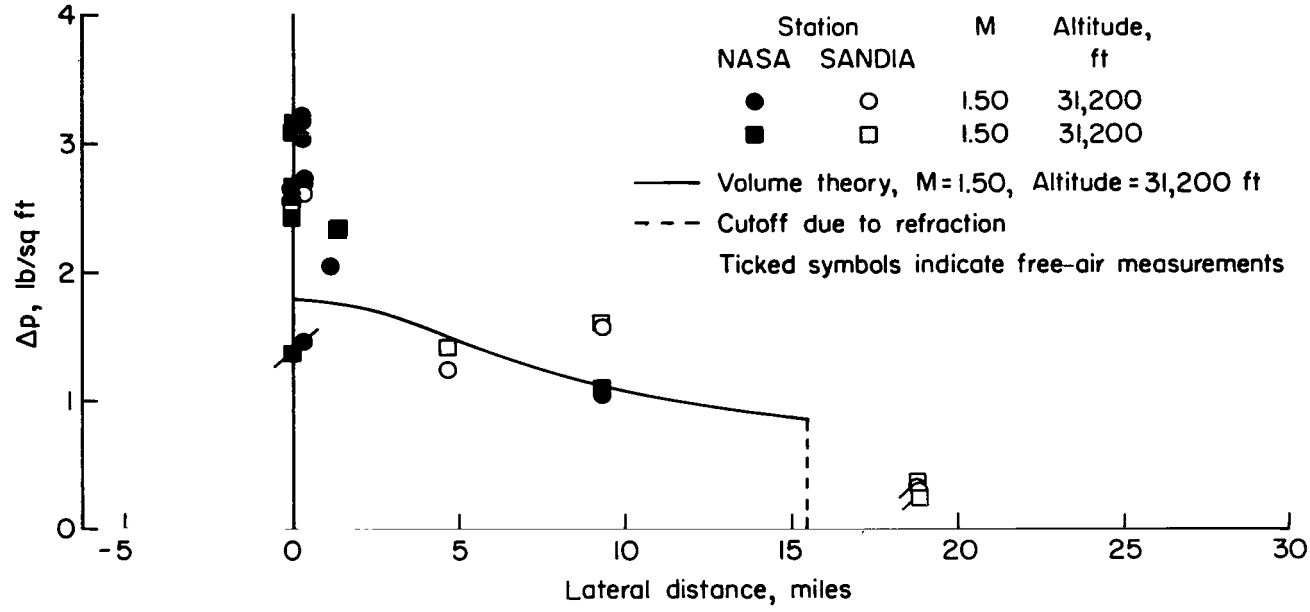

(a) Airplane A.

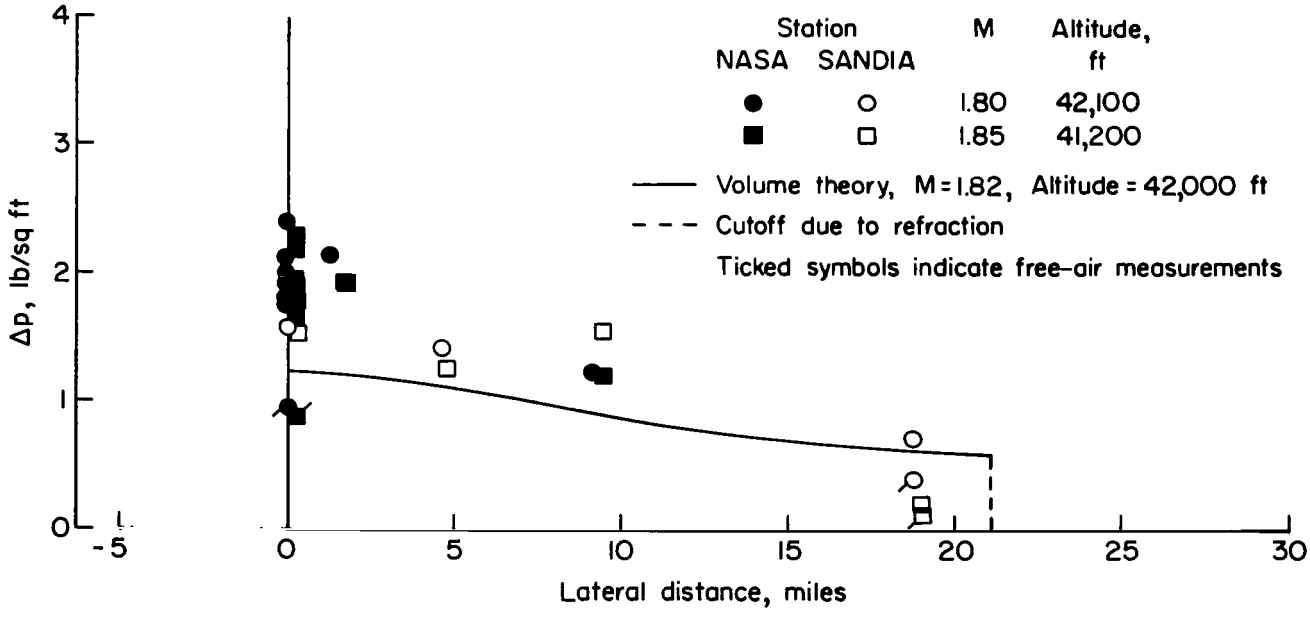

(a) Airplane A - Continued.

Figure 10.- Measured ground and free-air shock-wave overpressures for bomber airplane for a range of altitudes and Mach numbers as a function of lateral distance from ground track.

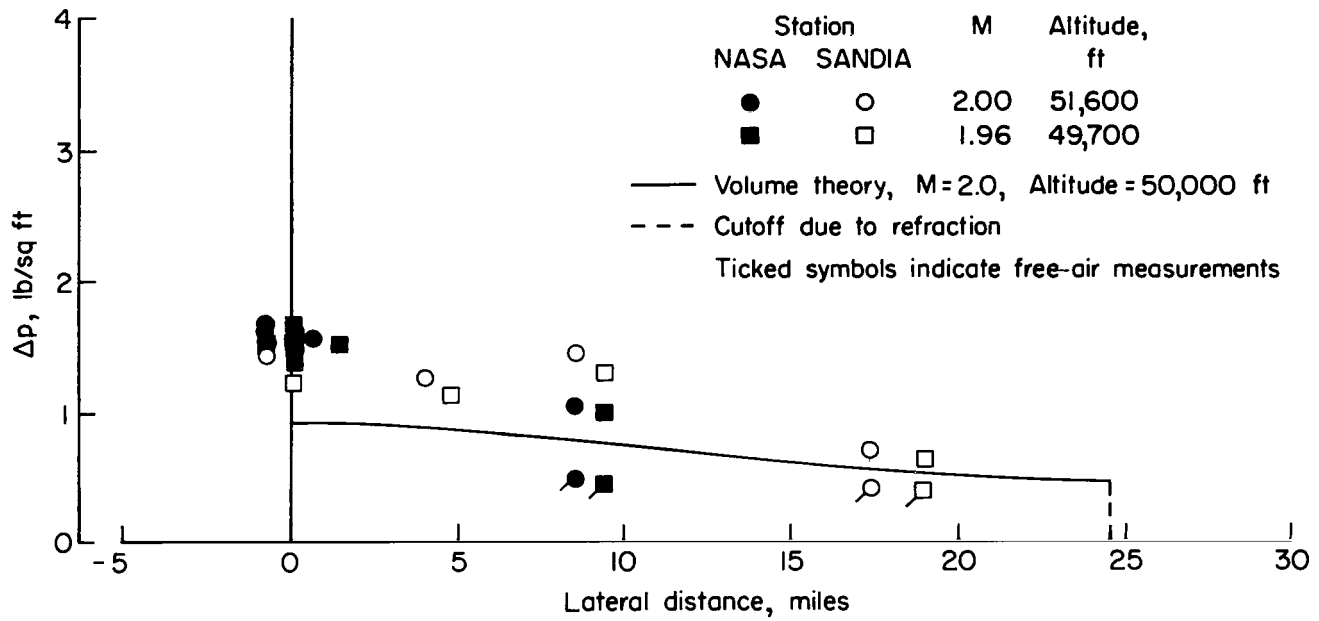

(a) Airplane A - Continued.

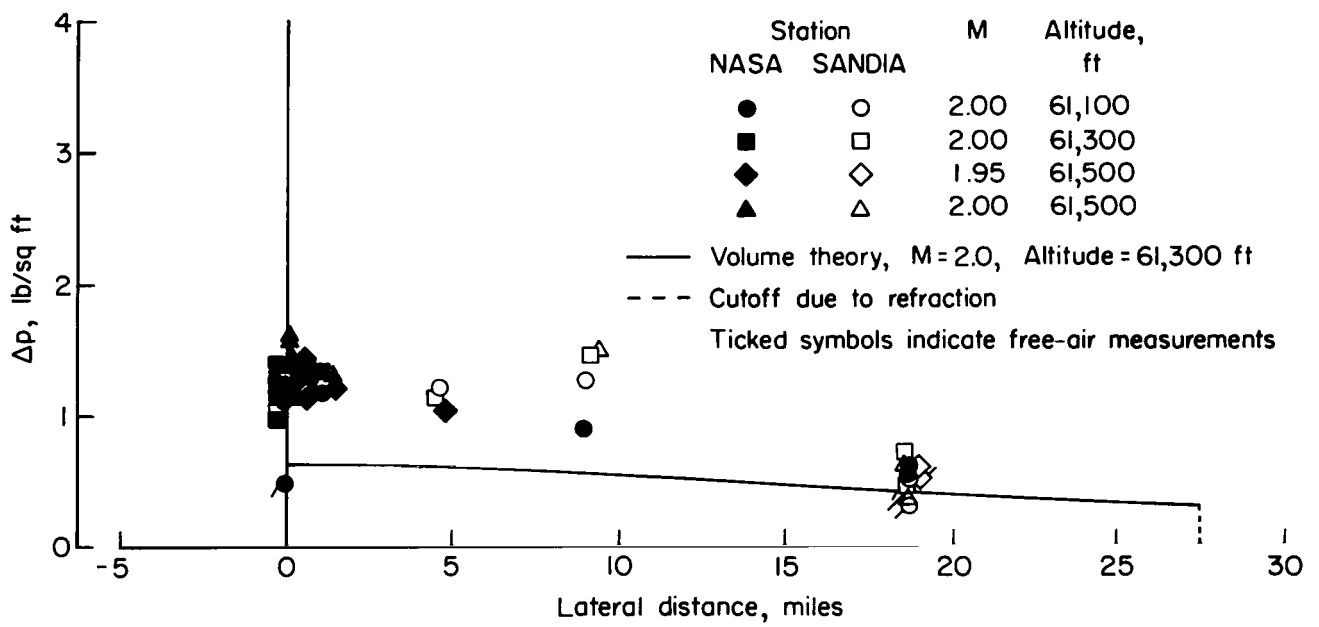

(a) Airplane A - Continued.

Figure 10.- Continued.

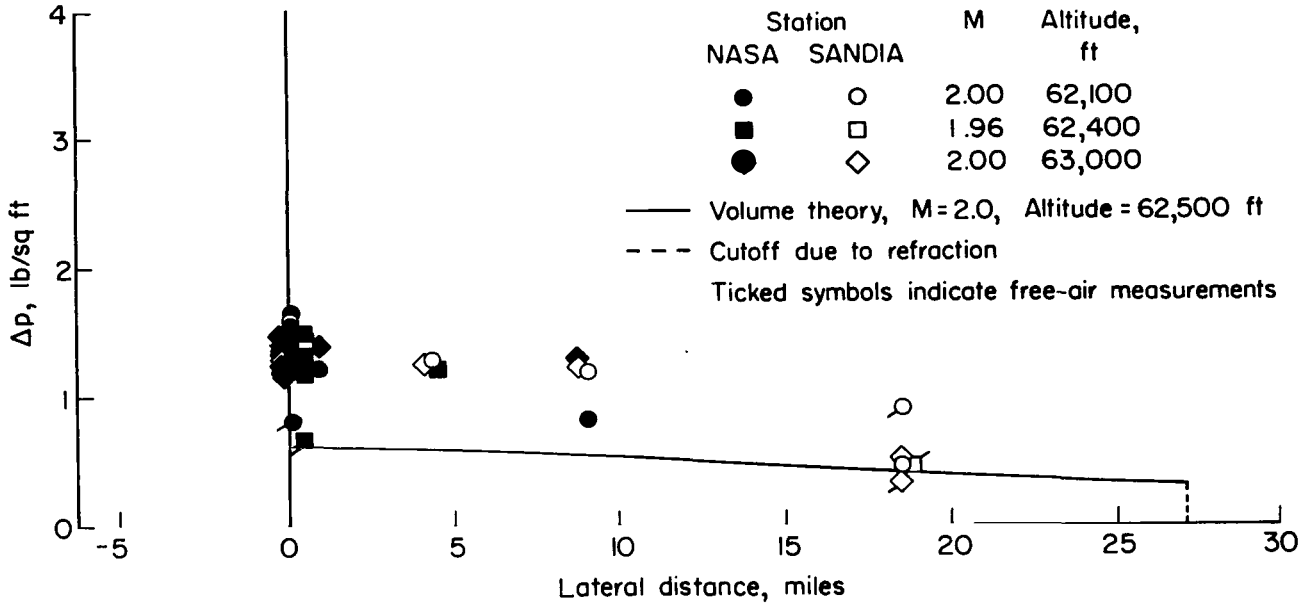

(a) Airplane A - Continued.

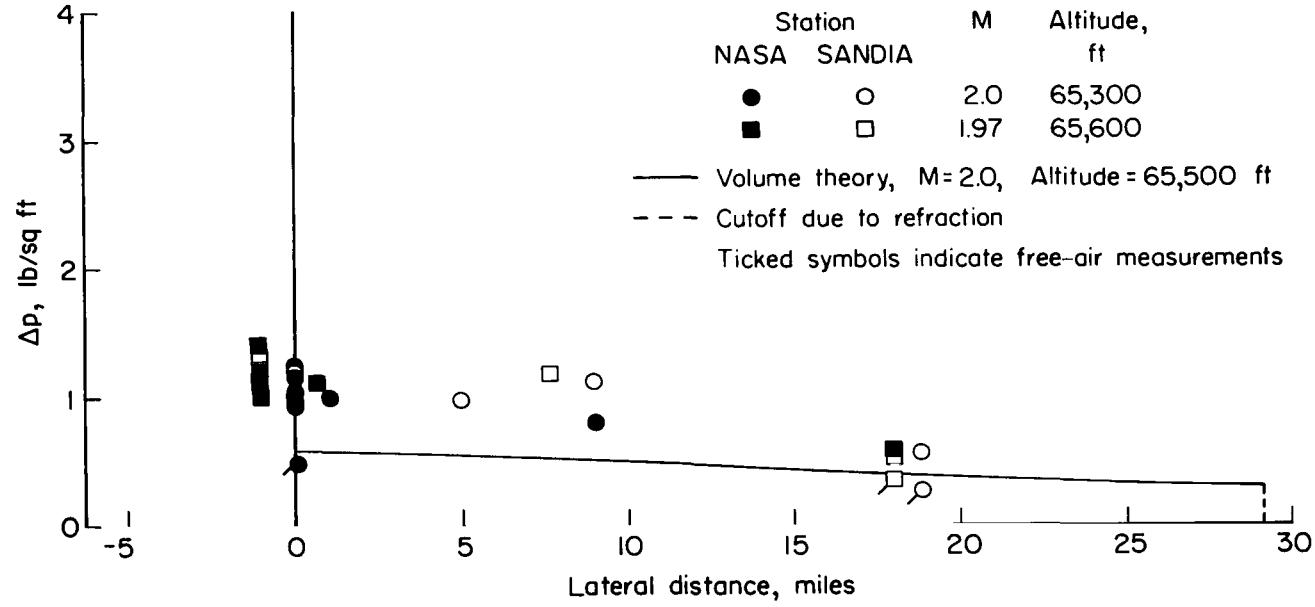

(a) Airplane A - Continued.

Figure 10.- Continued.

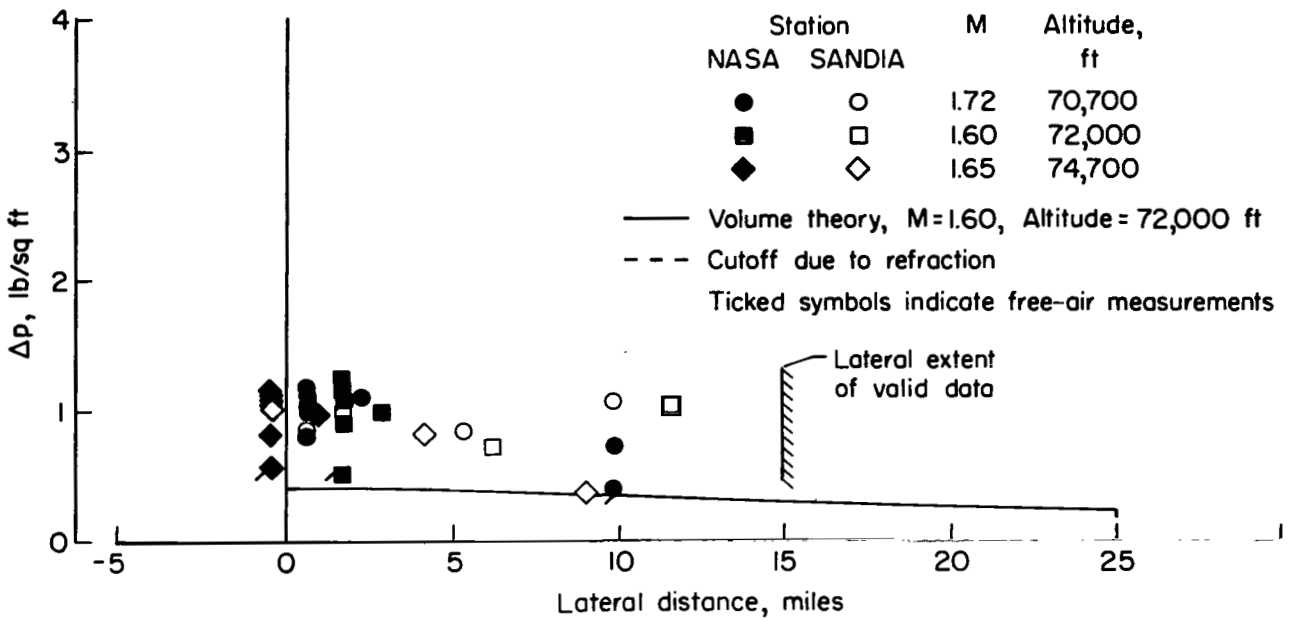

(a) Airplane A - Concluded.

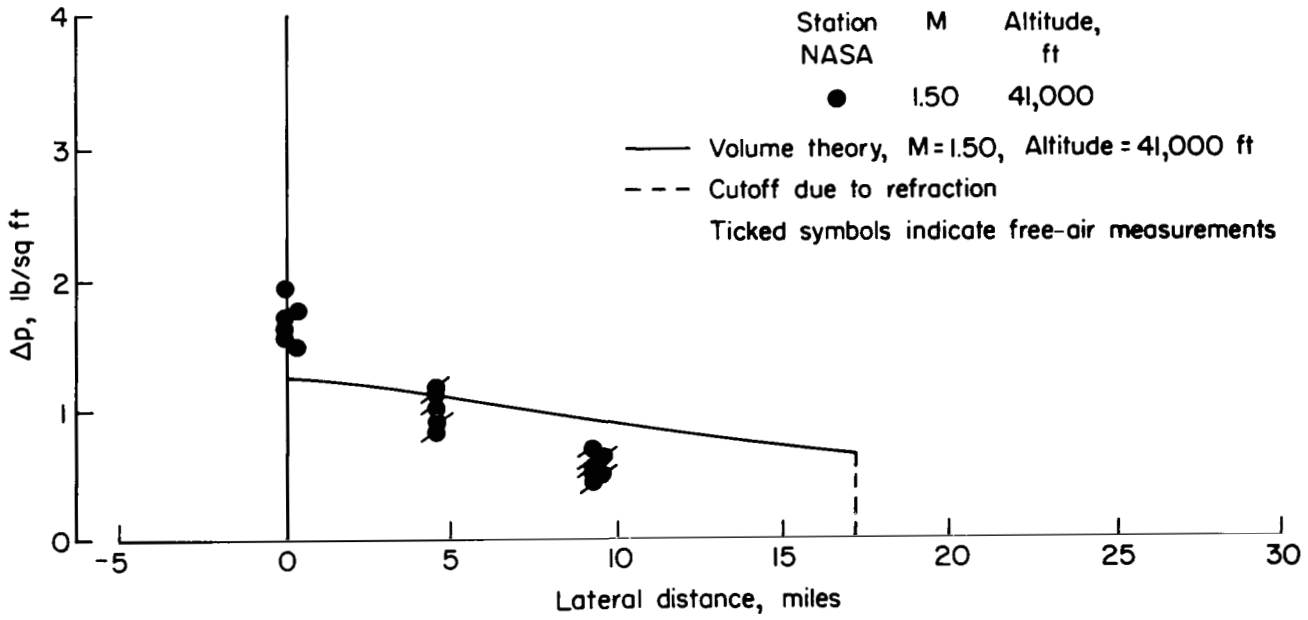

(b) Airplane A with pod.

Figure 10.- Concluded.

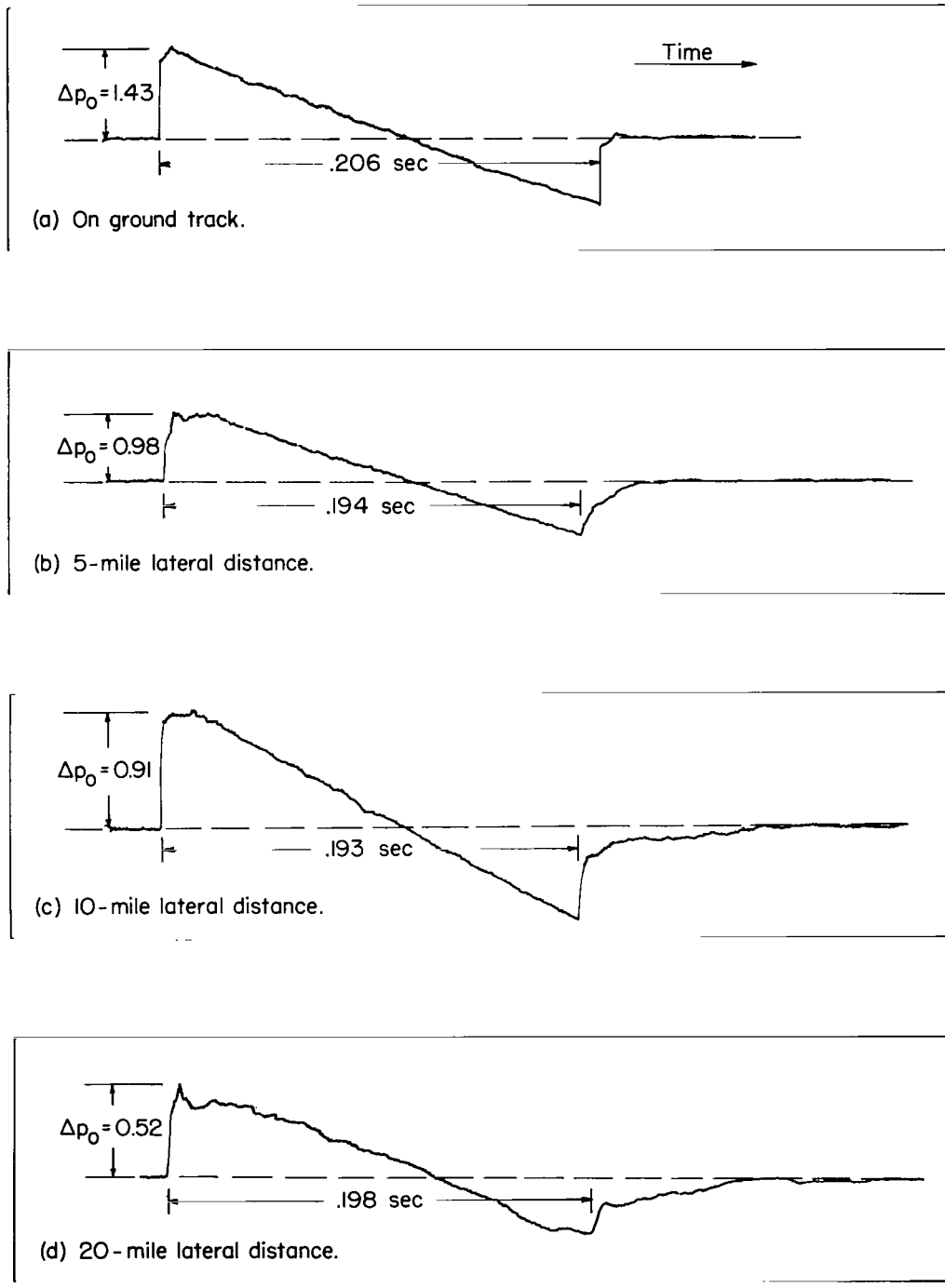

Figure 11.- Tracings of sonic-boom ground pressure signatures at various lateral distances from the ground track for the bomber airplane A at an altitude of about 61,000 feet and a Mach number of 2.0 (Δp_o in lb/sq ft).

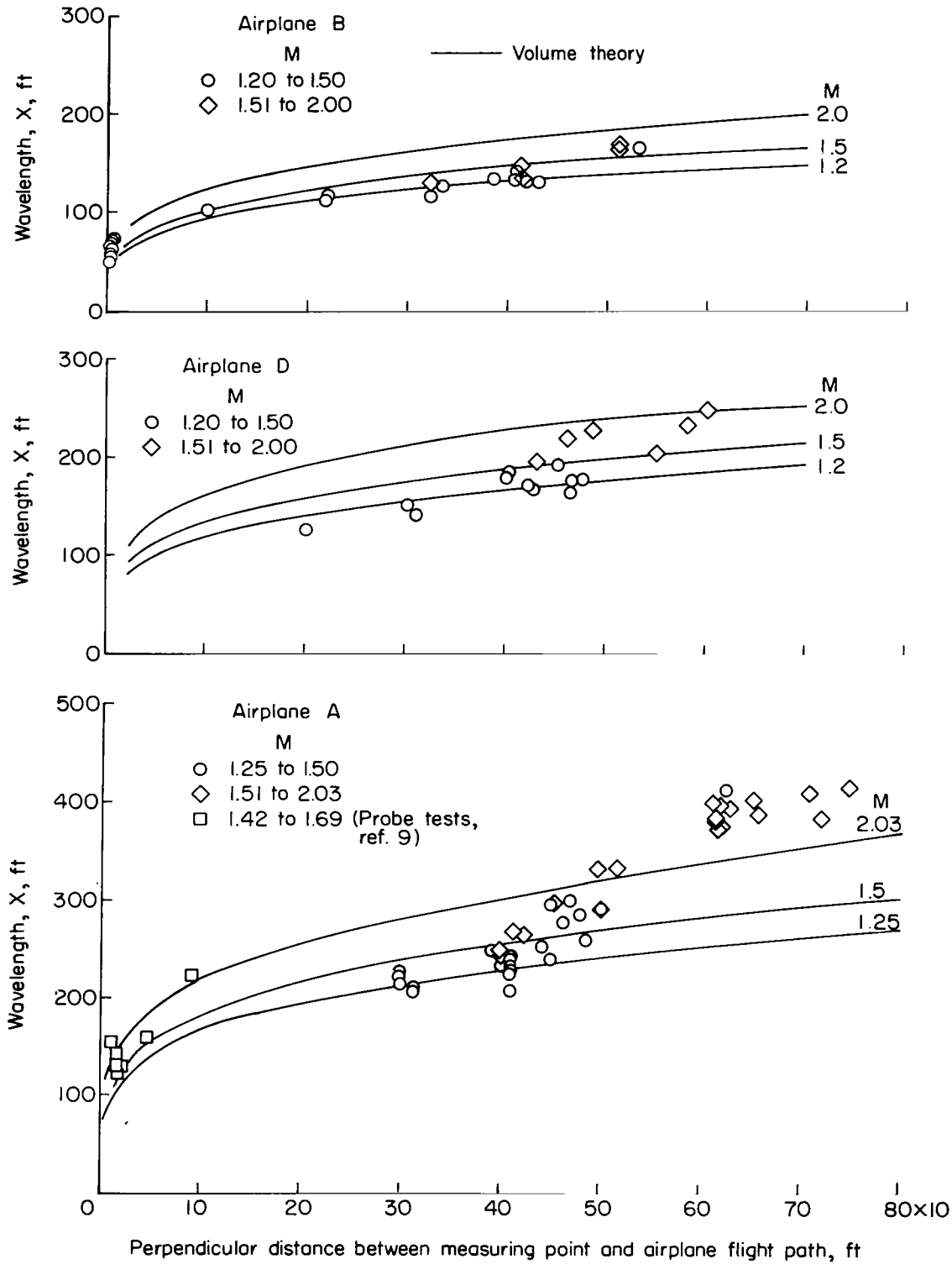

Figure 12.- Comparison of measured and calculated wavelengths.

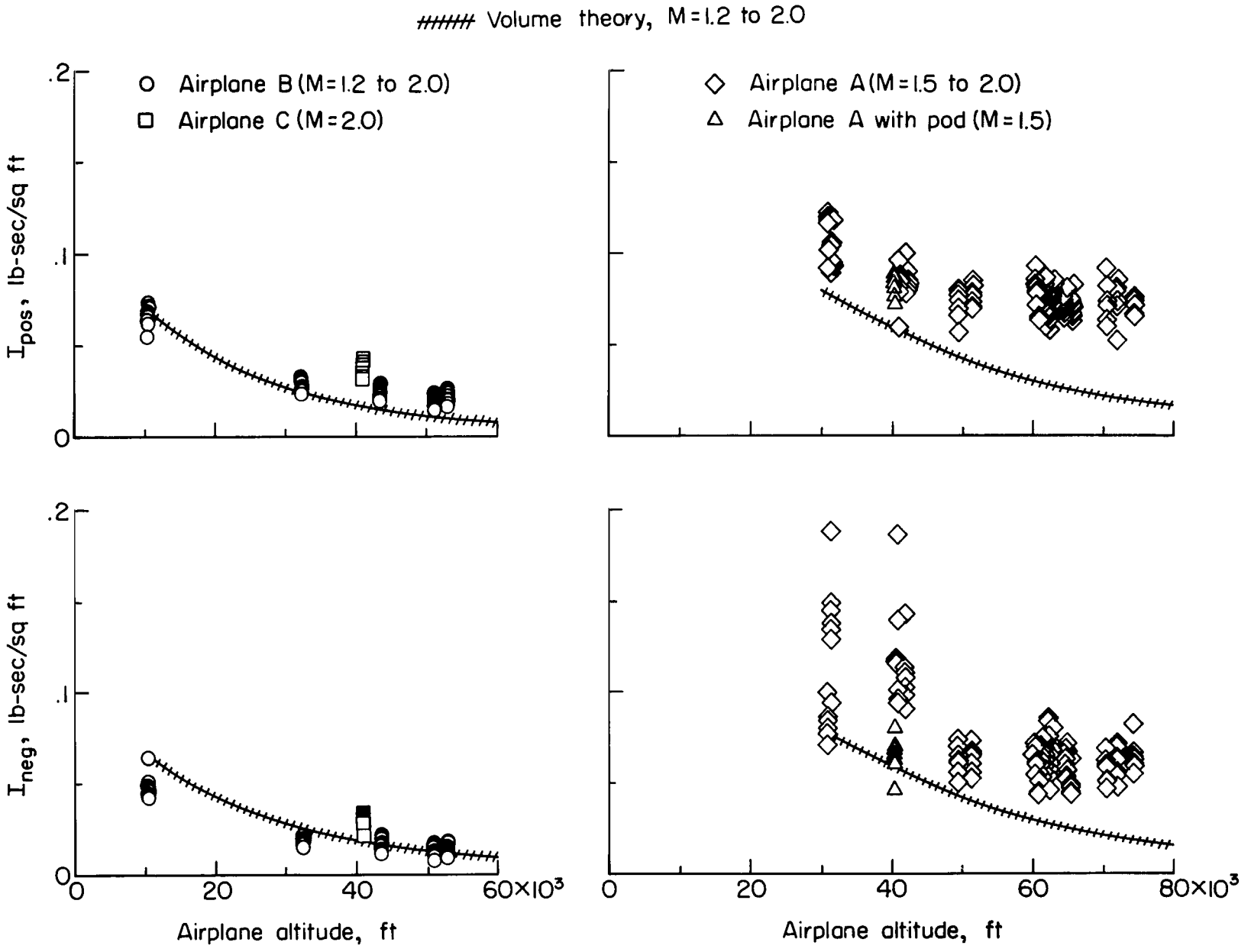

Figure 13.- Measured and calculated positive and negative impulse along ground track of airplane as function of altitude.

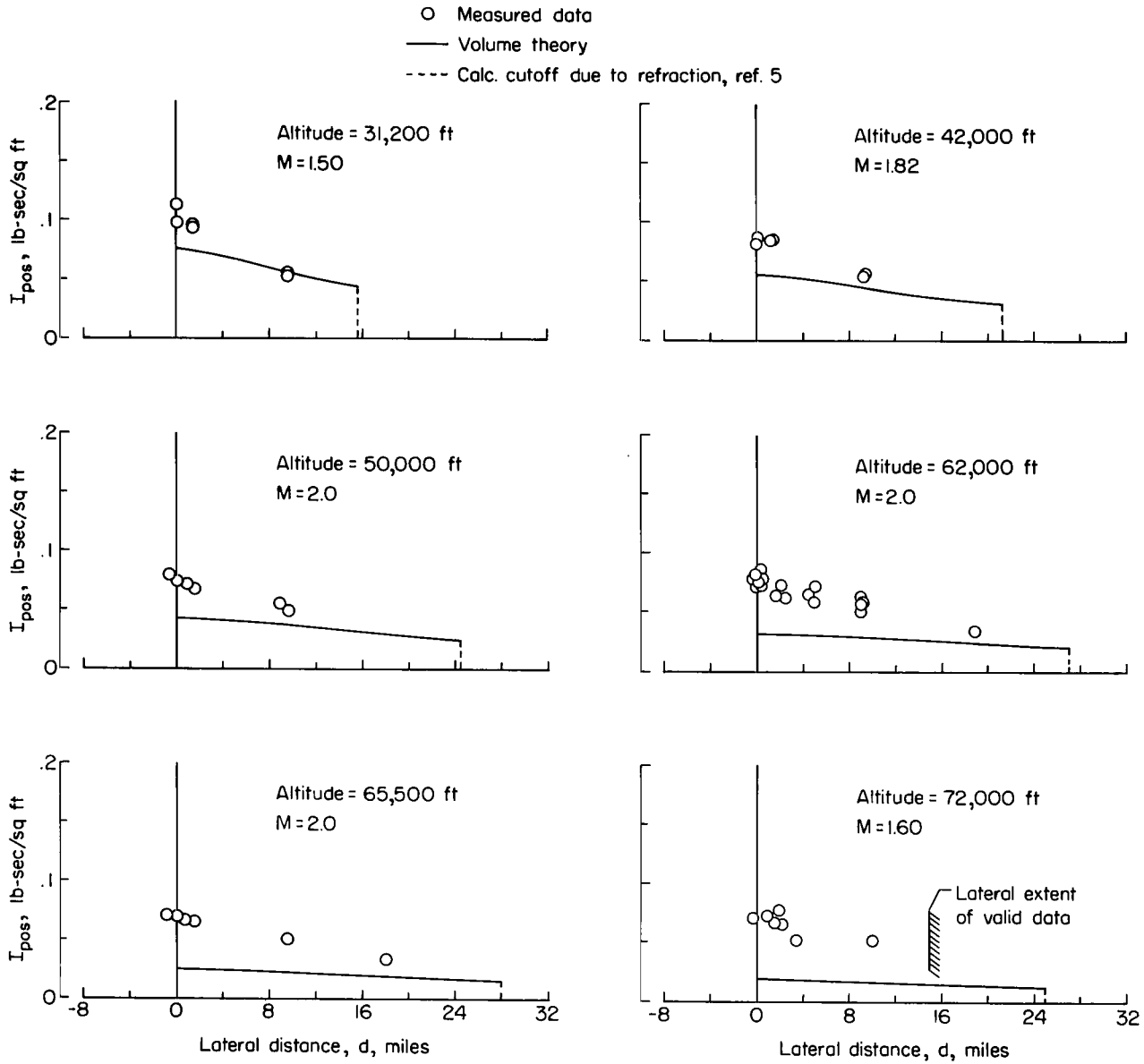

Figure 14.- Measured and calculated positive impulse from airplane A as a function of lateral distance from ground track.

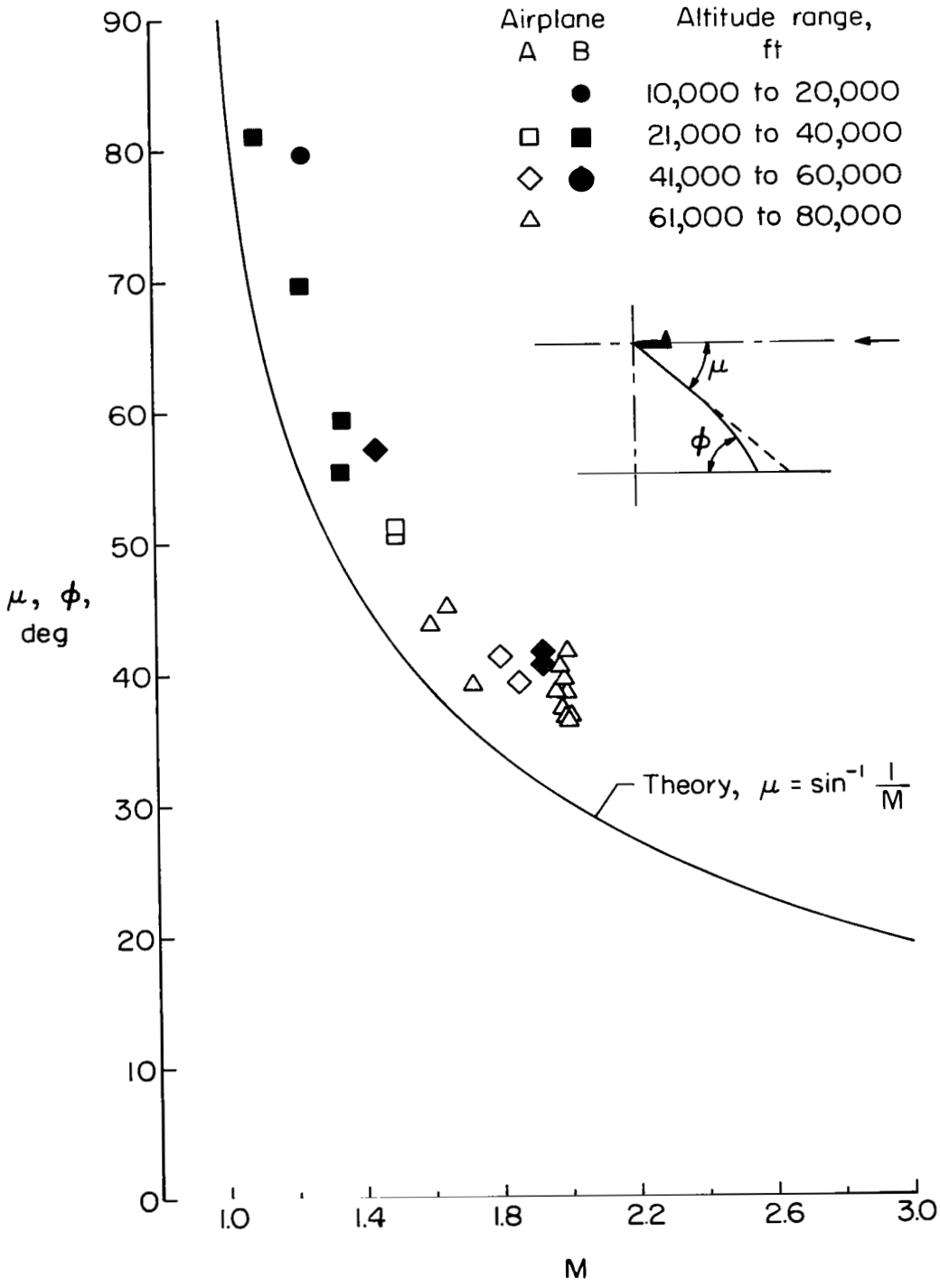

Figure 15.- Comparison of Mach angles and measured shock-wave angles at various altitudes and Mach numbers for ground-track conditions.

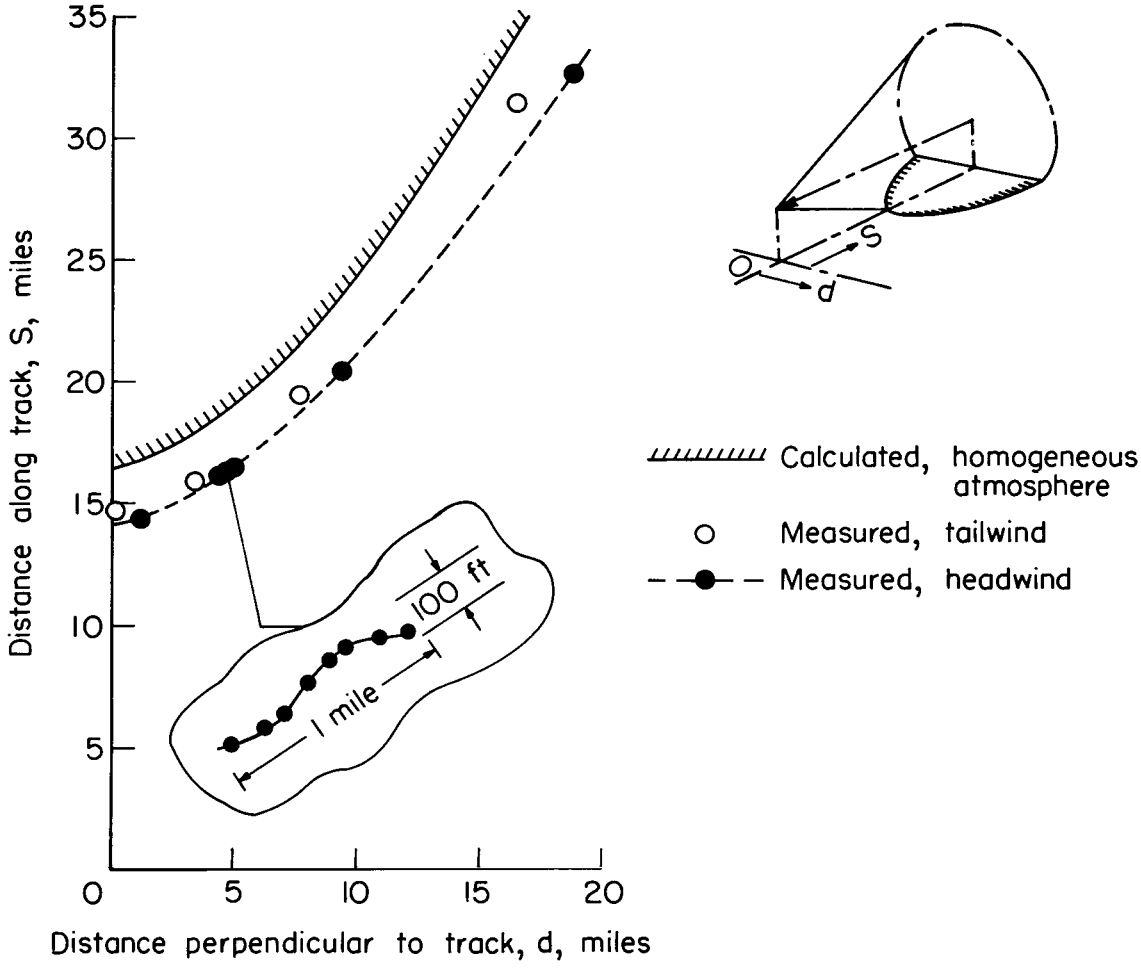

Figure 16.- Effect of atmosphere on sonic-boom wave front.

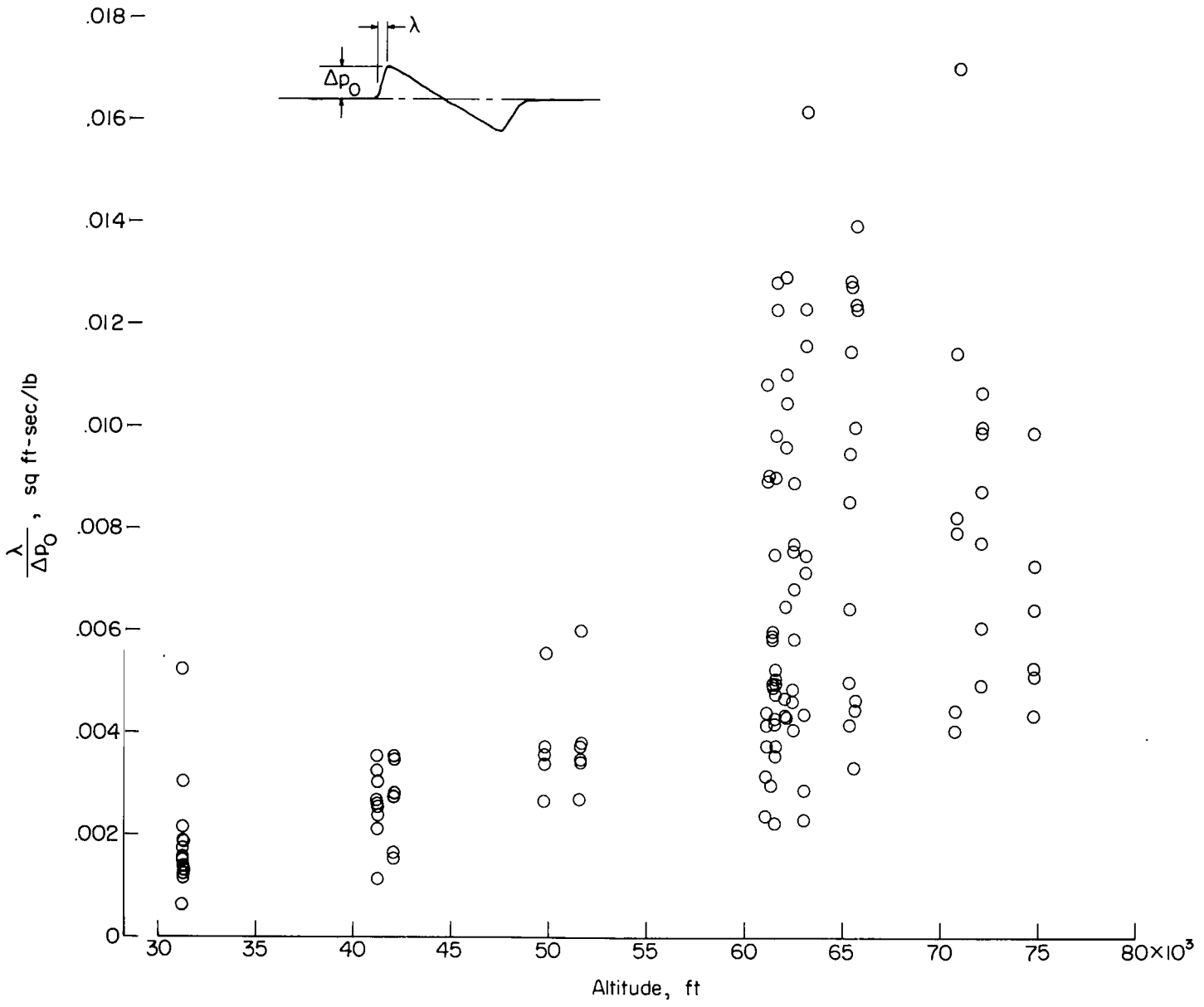

Figure 17.- Measured rise time obtained from sonic-boom pressure signatures along ground track as a function of altitude. (Data are for airplane A.)